Doc. No. 03-602-H7
Rev. 0 - JUNE 2005

ESA ESTEC
Noordwijk, The Netherlands

Bionics and
Space System Design

Energy Storage Structures for
Deployable Systems

D'APPOLONIA

ESA ESTEC
Noordwijk, The Netherlands

Bionics and Space System Design

Energy Storage Structures for Deployable Systems

Prepared by	Signature	Date
Raimondo De Laurentiis		
Donato Zangani		
Verified by	**Signature**	**Date**
Stefano Carosio		
Approved by	**Signature**	**Date**
Andrea Barbagelata		

Rev.	Description	Prepared by	Verified by	Approved by	Date
0	First Issue	RDL/DMZ	SMC	AB	June 2005

TABLE OF CONTENTS

LIST OF TABLES

LIST OF FIGURES

LIST OF FIGURES
(Continuation)

LIST OF FIGURES
(Continuation)

REPORT
FINAL REPORT

1 BACKGROUND

Biomimicry is a multi-disciplinary science involving a wide diversity of other domains like electronics, informatics, medicine, biology, chemistry, physics, mathematics, and many others. However, it is quite unusual to find key people or expertise centres that have cognition and expertise in all these disciplines as a whole. Therefore, there is a need for the establishment of a capillary network of contacts through Europe and elsewhere that will enable to reach also those academic centres, which are not much visible due to their reduced dimension or recent origin. Additionally, although some peculiar conditions characterizing space environments can be similarly encountered on earth (e.g. desert zones) and specific solutions found within these terrestrial contexts can be adapted to space conditions, there is a majority of cases, which are subject to conditions which are broadly different from those encountered on earth (e.g. gravity absence). Therefore, the biomimetic approach in the space sector results more complex and has to be considered in a multidisciplinary and cross-sectorial framework to overcome barriers. The problems to be addressed to exploit the potential of the biomimicry approach in the space domain can be summarized as follows:

- biomimicry has become a real science only in recent years and therefore there is no consolidated co-operation environment with space engineers;
- research in biomimicry across Europe and Canada and more generally at world wide level is scattered and fragmented, it is not easy to locate the proper academic experts for a given space application;
- biomimicry is a multi-disciplinary science and it requires several expertise which is difficult to locate in the same organization;

- some databases with information about possible natural phenomena, biomimetic products, ongoing biomimetic research, biomimetic researchers, published articles exist, but they lack a systematic and a large-scale exploration of the potential of nature in view of applications in engineering, especially as far as the space domain is concerned;

- in current knowledge-basis the abstraction of the biological functionality is missing, therefore solutions inspired by nature are sporadic and random-governed;

- space conditions are completely different from life forms habitats and space engineers are so far not fully aware of applications of biomimetics.

Therefore, the overall objectives of the study consists in the development of a co-operation platform between space and biomimicry experts in order to bridge current gaps that exist for an effective application of natural mechanisms and phenomena in space system design and to foster the development of a new generation of space systems. This has been achieved by:

- performing a comprehensive collection and review of information concerning attempts made since today in Europe and elsewhere in finding solutions through a biomimic approach, including an insight into planned research activities and trends;

- developing a detailed biomimicry knowledge map that allows to identify expertise and competencies in ESA member states and elsewhere;

- providing an overview of the unique characteristics and properties of various life forms found in nature (e.g. animals, plants, etc) and to ascertain whether these characteristics could be an inspiration to create innovative space systems;

- conceptualising several innovative space systems and components which incorporate the design, features and mechanisms of nature's life forms.

All the gathered information have been implemented into a database which is available online at www.bionics2space.org. The added value of the database is in the deep analysis made on each biological system described, supported by literature and reference articles, patents, etc.

The project group has then been focusing on the analysis of the information collected and on whether any of these biological principles might hold potential for application to the design of space systems or provide solutions to space-related technical challenges.

Therefore, the project group has identified twelve different cases in which the application of biological principles could bring a real added value to the solution of technical constraints within the space field. The identified case studies are reported below:

- deployable digging mechanism for sampling below planetary surfaces;
- energy storage structures for deployable systems;
- rigidisation of deployable structures;
- smart swarm on mars;
- robust biologically inspired navigation techniques;
- planetary exploration with free energy (based on sun flowers);
- adaptive and versatile biologically inspired locomotion control;
- balance between adaptability and stability;
- automatic self-assembly in space;
- landing and planetary exploration;
- energy storage structures for deployable systems;
- planetary exploration with free energy (based on dandelion seeds).

Such work has set the base from which a more detailed analysis has been performed: for each of the topics, a responsible among the Bionics Expert Team has been identified; such expert has been in charge of providing to the partners the assessment of the idea of application.

The results of such detailed analysis have been presented in the framework of the Bionics workshop held in ESTEC on November 2004. The output of such event has been the selection of four case studies which have been further assessed by proposing first attempts of engineering solutions inspired by nature. Such case studies are the following:

- energy storage structures for deployable systems;
- case study on adaptability versus stability;
- deployable digging mechanism for sampling below planetary surfaces;
- landing and planetary exploration.

In this report the work undertaken for the "Energy Storage Structures for deployable system" case study is described.

2 ENERGY STORAGE STRUCTURES FOR DEPLOYABLE SYSTEMS

2.1 INTRODUCTION

The overall objective of this case study is to assess the applicability of mechanisms and concepts for deployment of structures in nature to space applications such as the deployment of large antennas in orbit. The idea is to adapt the closure mechanism of the Venus Fly Trap to the deployment of structural booms in orbit. The use of smart materials such as shape memory alloys embedded in the structure of the boom is also assessed.

In the following paragraphs, an overview of the space requirements is reported together with a description of the current solutions exploited in space. Paragraph 2.4 provides a detailed description of the biological principle which can be of inspiration to find innovative solutions to the problem tacked. Moreover, Paragraph 2.5 provides with a first attempt of proposing an engineering solution.

2.2 SPACE REQUIREMENTS

2.2.1 Space Requirements

The successful performance of any structure depends largely on the identification of the critical or primary loads and design criteria on which the design is based. Space structures must be typically launched, deployed, erected, assembled or fabricated in space. Indeed, their primary design requirements will be derived from the spaceflight environment and will deal with phenomena which typically occur in such framework. The proper selection of critical design requirements it is not only necessary for the preliminary study of missions and concepts so that realistic structural data can be generated for cost and feasibility analyses and for the determination of technology readiness (NASA, 1981). The rational design of all structures must start with a definition of the task or function of the structure. For space structures which have to be deployed in orbit, the environment in space is quite benign, the applied loads are apt to be small, and the strength of the structure is not a pacing factor. On the other hand, the demands of antennas and solar reflectors for accurate positioning and the

requirements of adequate stiffness to avoid undesirable structural distortions are often serious and thereby dictate the design. Moreover, for deployed structures another primary requirement is that the structure must be packaged in the available volume for transport to space.

Damage tolerance is clearly a requirement. Large expanses of statically determined structure with thin members may have an unacceptably high probability of failure due to meteoroid damage. Even if the structure were redundant, the degradation in precision caused by local damage must be considered.

Identification of critical design requirements requires consideration of five phases in the life of the a space structure:

- Prelaunch;
- Launch;
- Interorbit boost;
- Deployment in space;
- Space operation.

The prelaunch phase influences the design primarily through the requirements on fabrication accuracy and ground test. The launch phase influences the packaged configuration. Interorbit boost can cause major design loads if the structures is previously erected. The integrity of the partially deployed structure must be assured. Finally, the structure must furnish secure and precise support to the payloads during the long operational phase. Indeed the most basic requirement is that the structure must well interface with its payload and the other parts of the system. The requirements of dimensional precision and high stiffness are very important.

2.2.2 Precision Requirements

Many of the possible missions involving large space structures require a very high precision in the structural geometry. Not only must the structure be stiff enough to avoid unwanted

distortions, but also the structure must be constructed accurately and in such a way as to retain its accuracy during the long exposure to the variable temperature, ionizing radiation, high vacuum space environment. Of course, careful adjustment in space during deployment and meticulous maintenance is one possible strategy to follow. But a great deal of time, money and complication can be avoided if the precision requirements could be met without adjustment in space and without maintenance.

Relevant research efforts have been focussing on such approach. Much attention was devoted to the estimation of the effect of unavoidable tolerance errors in the dimensions of individual structural elements on the accuracy of the overall structure. This investigation was supported by the equivalence principle linking the analyses of errors to that of vibration frequencies. In Figure 1, the achievable size D of an antenna, measured in radiofrequency wavelength λ, is plotted versus the rms value of the unit length error of the structural elements. The rms distortion of the antenna surface is taken to be $\lambda/100$ and the results apply to a ratio of focal length to structural diameter off two. The curves show that the truss structure is most attractive and that $D/\lambda = 10{,}000$ is possible for fabrication-error parameter of 10-5, which should be obtainable with careful tooling (NASA, 1981).

Not only the structure must be deployed accurately, but also it must remain accurate. Therefore, attention was given to the effects of thermal strains which are expected to be the major contributor. The conclusion is that very precise structures are possible at reasonable cost. Such precision is possible because the structures are designed to be deep enough to avoid the magnified surface errors that come from shallow configurations.

Finally, the materials used in the structure must have excellent dimensional stability. The deepness of the structure keeps the demands on material performances to reasonable levels, but the effects of differential thermal strains and long-terms changes must be kept to a few parts per million (NASA, 1981).

2.2.3 Member Slenderness

The operational loads in well-designed space structures are so small that the members sized to carry the resulting internal loads are likely to be very slender. Realistic sizing must therefore come from other considerations discussed in the following.

An important criterion arises from the fact that axial stiffness of a strut is severely degraded if it is not straight. As seen in Figure 2, the reduction in stiffness is a function of the ratio of the crookedness δ to the radius of gyration k_c of the cross section. The equation shown in the figure applies to a sinusoidal deformation shape. Other shapes such as constant curvature and gravity-sag shapes yield closely similar results. In order to maintain the loss in the axial stiffness to 5%, let the crookedness δ be set at less than k_c /3. For a thin-walled tube, the ration between δ and the diameter d must be less than about l/10 (NASA, 1981).

Such straightness demands are easy to meet for ordinary proportions. As the slenderness ratio of strut length l to k_c increases, however, practical difficulties arise. The consequences of some of these difficulties are shown in Figure 3.

As previously remarked, ground testing will be required. In order to avoid the complications of supporting each strut at interior points against gravity sag, the gravity deflection:

$$\delta = 5/384 \times [(\rho g l^4)/(E k_c^2)]$$

must be kept small enough. For material properties appropriate to graphite composites,

$E = 1.1 \times 10^{11}$ N/m^2
P = 1520 Kg/ m^3

the slenderness limitation given on the first line of the figure must be observed (NASA, 1981).

Measuring the crookedness of slender fabricated members is a well-know problem. While testing in a horizontal position is a possible approach, questions always arise about the effects of the supports on the validity of the data. A preferable approach is to suspend the strut vertically for measurements. In order that the data be valid, the ratio of gravity-induced load to Euler load:

$$P/P_{eu} = [\rho g l^3 / \pi^2 E k_c^2]$$

must be small. This results in the criterion on the second line of Figure 3.

The third criterion arises from the difficulty of fabricating the member with enough straightness. Too stringent a requirement could result in a high rejection rate. The rise height of a fabricated member would be:

$$\delta = [l^2 \Delta\varepsilon / 8k_c]$$

where $\Delta\varepsilon$ is the differential strain error arising, for example, from nonuniformities of material properties or curing temperatures in a distance kc across the cross section.

Where the struts are assembled into a redundant structure, the length imperfections will induce residual loads in the struts. The conclusion is that the rms residual load strain is equal to the rms unit member length imperfection σ_ε divided by 3^1/2. The ratio of the rms member load to its Euler load is:

$$P_{rms} / P_{Eu} = [(\sigma_\varepsilon / 3^{1/2}\pi^2)(l/k_c)^2]$$

The resulting limitation is given in the fourth line of Figure 3. As a final example of slenderness limitation, the natural vibration frequency of the member should be higher than that of the structure as a whole. For a pin-ended member and free-free truss with square planform, the ratio of the strut and truss natural frequencies is (NASA, 1981):

$f_{strut} / f_{truss} = 3{,}43\ [(1+mp/ms)k]^{0.5}(L)^{2}K_c/(Hl^2)$

where mp/ms is the ratio of the payload mass to the structural mass and k is the joint-mass factor. The resulting slenderness criterion is shown on the last line of Figure 3.

Comparison of these limitations shows that ground testing requirements could predominate. If these are accounted for in some other fashion, then the residual-load criterion would be most severe (NASA, 1981).

2.3 STATE OF THE ART

2.3.1 Deployable Booms for Solar Arrays

Deployable space structures play traditionally an important part in the realization of space missions since the limited envelopes of the existing launchers constrain the payloads geometrically. Increasing demands, for example for energy supply, require more and more very large appendages. Power generation of the International Space Station (ISS) is provided by eight deployable solar arrays, each spreading an area of approximately 32.6m to 11.6 m. The 60m long boom which was deployed and retracted in 2000 on board of the Space Shuttle Endeavour during the Shuttle Radar Topography Mission (SRTM) is another prominent example. Presently, a clear trend for an increasing need can be identified for a number of future space structure applications like instrument booms, antennas and reflectors, Solar Sails, and huge solar space power systems. European space industries are increasingly harmonized by ESA's European Space Technology Master Plan (ESTMP). The need for key technologies is identified and development activities are envisaged to be supported by the establishment of research programs. In 2000, for example, solar arrays and synthetic-aperture radar (SAR) technologies were harmonized. Both are potential fields of application for deployable structures and the initiation of the harmonization of inflatable systems and deployable booms in 2003 clearly indicate the increasing need for deployable space structures development. The DLR Institute of Structural Mechanics contributes an assembly of four deployable ultra-light

carbon-fibre reinforced booms to the Solar Sail project (Figure 4). In its expanded configuration the boom assembly provides the supporting structure for the tightening of the flexible sail membrane (Sickinger et al., 2004).

The structural boom design is based on requirements that were determined during a Solar Sail ground demonstration. Although only 14-meter long booms were built during this demonstration phase (Figure 5), the design was worked out according to future mission applications for a length of 28 meters. The cross-section geometry definition results from a mass optimization while fulfilling a certain minimum bending stiffness requirement and geometrical constraints. Finally, the specific mass of the booms amounts to 100 grams per meter only. Following the lightweight philosophy of the boom design, the internal energy of the booms, which is stored during the packaging procedure, can also be used for the deployment. The self-deployment test depicted in Figure 6 — completely driven by elastic deformation energy—takes only 10 seconds. However, a controlled and guided deployment or a retraction of the boom require therefore special mechanisms. For the Solar Sail application a deployment module is developed, which contains and latches the boom assembly in stowed configuration and guides the deployment sequence.

2.4 BIOLOGICAL PRINCIPLE

Plants are not known for their ability to move quickly. Nevertheless rapid plant movements are involved in essential functions, such as seed and pollen dispersal (exploding fruits in Impatiens, squirting cucumber and trigger plants), defence (sensitive mimosa) and nutrition (Venus flytrap, Dionaea muscipula or Aldrovanda vesiculosa, bladderwort). Of these spectacular examples that have long fascinated scientists, the leaves of the Venus flytrap (Figure 7), which snap together in a fraction of second to capture insects and other small animals which venture onto its trap leaves and trigger their closure by disturbing certain sensitive hairs, have long been a paradigm for study.

Darwin (1875) thought that the midrib of the trap is a hinge (which it isn't); Ashida (1934) and von Guttenberg (1959; 1971) suggested that the upper epidermis loses turgor and shrinks;

Williams and Bennett, (1982) proposed that the cell walls of the lower epidermis soften and stretch under turgor pressure. Hodick and Sievers (198) concluded that any mechanism which requires a physiological (e.g. turgor change) will be too slow. It seems obvious that the only type of mechanism which can provide the speed is elastic, *using stored strain energy provided by turgor pressure*[1]. This has the advantage that the turgor and mechanical properties of the cells and tissues do not need to change during the fast phase of closure, though such changes probably occur in the earlier phases (Vincent, unpublished) and certainly in the later phases of closure (Fagerberg and Allain, 1991).

Jeronimidis and Parkyn (1988) have studied the bistable curvature in a prestressed sheet of material with three 1ayers, showing that it is possible for a plate to change shape from one curvature to another (equivalent to the fly trap leaf being open or closed) without any change having taken place in the elastic properties (e.g. stiffness) of that plate. With the model system the shape change is elastic and reversible; often it is symmetrical, requiring the same forces and displacements to flip it from one curvature to the other. However, it is possible to construct a plate in which the behaviour is not symmetrical and the plate is stable in one configuration but only just stable in the other. This would be equivalent to the closed and open positions of the leaf, respectively. Thus it is possible for the fly trap leaf to go from a quasi-stable open position to a stable closed position without any change of its elastic properties, and any arguments about turgor not being fast enough are irrelevant since turgor need not change in order for the mechanism to function.

---

[1] In nature all processes and systems try to get to a stable situation (a balance). Inside a plant cell, there is a relatively high concentration of sugars and salts. Usually, on the outside of the cell there is a lower concentration of salts and sugars than the inside, except where plants are growing in sea-water. Since nature tries to reach a balance, water will move (diffuse) into the cells to try to lower the concentration of salts and sugars on the inside. This will result in an increase in the plant cell volume. Since plant cells have a wood-like cell-wall around them, they can not increase in volume indefinitely, as is the case with mammalian cells. The cells will push against the cell-wall and build up tension (turgor pressure). You can compare this with inflating a bike-tire. The inner tire is filled with air (water in plantcells) and pushes against the outer tire, which will not expand much if at all.

As Darwin had already noted, the leaf is curved outward (convex) in the open state and curved inward (concave) in the closed state. The leaf shape can be naturally characterized in terms of its spatially averaged mean curvature (k_m) and its spatially averaged gaussian curvature (k_g), both of which are invariant under rigid body motions and are thus indicators of shape. The snapping motion is characterized by three phases: a slow initial phase (20% of total displacement in 1/3 s), a rapid intermediate phase (60% of total displacement in 1/10 s) and finally a second slow phase (20% of total displacement in 1/3 s). The existence of the three phases is consistently observed, but the quantitative values may vary. Most of the leaf displacement occurs in the intermediate phase, during which the leaf geometry changes from convex to concave. Forterre et al. (Forterre et al., 2005) have observed that the averaged gaussian curvature is not constant during leaf closure, and also that it changes slowly and then rapidly as it passes through a minimum (Figure 9). As changes in k_g correspond to stretching the mid-plane of the leaf, these observations imply that closure is characterized by the slow storage of elastic energy followed by its rapid release. The maximum strain perpendicular to the midrib (direction x, in the plane of Figure 10 and Figure 11) is six times the maximum strain parallel to the midrib (direction y, in the plane perpendicular to that one of Figure 10 and Figure 11). Furthermore, the strains on the inner surface of the leaf are $\leq$1%, implying that closure is triggered primarily by differential strains in the x-direction. It is possible to validate this observation by cutting recently-closed leaves to determine the residual strains in them. Cutting a closed leaf in the x direction eliminates the constraining effect of curvature in the y-direction and allows it to recover its natural curvature in the x-direction, k_{xn}, Similarly, cutting the leaf in the y-direction allows us to observe the natural curvature in the y-direction, k_{yn}. We see that k_{xn} reverses sign during closure, but k_{yn} does not. This is consistent with previous observations and provides quantitative evidence that a change in k_{xn} drives leaf closure. Evidence supporting a mechanistic basis for this anisotropic deformation comes from microscopic examination of the leaf surface; the cells on the outer surface are highly elongated in shape, with their long axis oriented along the x-axis. As the cylindrical cell wall is reinforced azimuthally by microfibrils, it follows that any changes in turgor would lead to

deformations that are primarily in the x-direction, consistent with the observation that k_{xn} changes much more than k_{yn}.

Although the molecular and cellular processes underlying the water movements that control anisotropic curvature changes remain poorly understood, we now argue that the macroscopic mechanism of closure is determined solely by leaf geometry. For a doubly-curved leaf (one that is curved in two orthogonal directions), bending and stretching modes of deformations are coupled, meaning that bending the leaf causes its mid-plane to be stretched. If the coupling is weak, the leaf can change its shape from open to closed by varying its gaussian curvature and stretch without a large energetic cost. In such a situation, the leaf deforms smoothly to accommodate the change in k_{xn}. If the coupling is strong, the leaf will not deform much (owing to the large energetic cost of stretching its mid-plane), until eventually the change in k_{xn} becomes so large that the leaf snaps shut rapidly.

Following this initial, high-speed, phase the leaf continues to move, but more slowly. Although the leaf can be bent back into the open position, it has not retained its behaviour as a bistable and quickly closes again, suggesting that the redistributed stresses are relaxing due to alterations in turgor pressure and possible changes in the stiffness of the cell wall. The leaf will, however, open naturally over a period of hours, necessitating a different mechanical pathway. During this opening phase the leaf grows suggesting that the cell walls have reduced in stiffness and expand under turgor. This softening preludes generation and storage of strain energy, which is necessary for the leaf to attain its pre-closure state. It also means that the leaf does not have to cross an elastic instability in order for it to attain the fully open state. Only when it has completely opened can it afford to reinstate the prestrain and generate the necessary elastic strain energy. One can encapsulate this information in a conceptual model based on catastrophe theory. Catastrophe theory, introduced by Thom in the 1960s, is a mathematical formalism for modelling nonlinear systems whose behaviour is determined by the actions of a small number of driving parameters. In particular, it applies to systems that undergo either gradual or sudden changes in behaviour due to gradually changing forces. It has been applied to many problems in mathematics, physics and the social sciences. Thom

called the sudden changes that take place in a system "catastrophes" and developed a theory as a method of analyzing and classifying these changes (Figure 12). Thom's theorem asserts that the stationary state behavior of all systems that have up to four control parameters (or input variables) and two behavior (or output) variables, and which also have an associated potential function, can be described using one of seven elementary catastrophes.

In fact, if there is there is only one cause and one effect there is only one shape of catastrophic jump - the fold. If there are two controls and two effects there are only two shapes: the fold and the cusp.

A similar situation where plants exploit an internal prestress effect is found in plant stems. To begin at the beginning a plant needs light and therefore the plant needs to have a stem which is as high as possible per unit of metabolic cost. The stem has to support a variety of mechanical loads. The most important is the side loads due to wind; stresses arising from the weight of the plant itself are trivial by comparison with the bending stresses induced by drag forces. The plant stems must therefore be stiff to stand erect and it is limited by its ability to withstand to compressive forces experienced on the concave or compression face when it bends. It is highly unlikely that any plant will fail on the tension side since cellulose has a very high tensile strength. The most likely mode of failure is local buckling of the fibres in the cell walls, leading to a compression crease at the macroscopic level. The fibres buckle because they have little or no lateral support.

Rigidisation mechanisms in plant stems seems to be related to the existence of pre-stresses due to turgor effect.

2.5 PROPOSED ENGINEERING SOLUTION

The proposed engineering solution relies on the use of SMA Hybridized Fibre Thermoplastic matrix laminates to make bistable tubular extendable members with embedded actuations. Adaptive structures, showing the ability to change their inherent properties in response to an applied field, utilize smart materials such as piezoelectric, magnetostrictive, electrorheoligical

fluids, magnetorheological fluids, and shape memory alloys (SMAs). Amongst these SMAs have the ability to undergo large deformations, to change shape, stiffness, natural frequency, damping and other mechanical characteristics in response to a change in temperature and stress. They exhibit two unique phenomena known as shape memory effect (SME) and pseudoelasticity.

The amount of recoverable strain that can be obtained when the SMA is transformed from its plastically deformed martensite phase (low temperature) to its elastic austenite phase (high temperature) can be up to 8% for Nickel-Titanium alloys, but a more workable range is 3-5%.

Potential for applications in self-erecting structures, thermally actuated devices, and energy-conversion systems was identified by Buehler and Wang. Other potential applications include damping or energy absorbing devices, thermally actuated couplings and fasteners, and biomedical devices. Wayman and Otsuka (Otsuka and Wayman, 1998) gave more detailed descriptions of specific devices such as pipe couplings, thermostats, a robot hand, and various biomedical systems.

A possible approach to adaptative-morphing structures is the integration of thin shape memory alloy wires in composites. Several authors have studied structural configurations using both externally attached SMA wire as well embedded SMA wire. In particular the works of Lagoudas and Tadjbakhsh (Lagoudas and Tadjbakhsh, 1992) and Rogers et al (Rogers et al. 1989) represents milestone works.

The potential advantages of hybridising the composite structures with SMAs fibres or SMA strips, comprise:

- prestraining of the structure in order to raise the critical buckling load;
- embedded actuation (i.e. change from a stable situation to another stable situation passing through a catastrophic point);

- activation of deployment (i.e. potentially it would be not anymore required to stowe the structure in a deployment mechanism to prevent the uncontrolled release);
- vibration damping (highly desiderable in combination with large space structures with very stringent precision requirements);
- structural/deployment control.

Bistable tubes are split tubes with essentially the same geometry as a carpenter's tape; however, unlike a carpenter's tape, which is only stable when extended, these structures have a second stable state, they are also stable when coiled (Figure 13).

There are two ways to make a tube bistable; either by altering the bending stiffness of the structure so that it is no longer isotropic, for instance by using a fibre-reinforced composite, or by setting up an initial prestress in the structure. Tubes with different lay-up form coils of different radii.

Storable Tubular Extendible Members (STEMs) have been invented in Canada in the early 1960's as application for deployable booms. The thicknesses of all these structures is sufficiently small that they are deformed purely in the elastic range when they are folded and a large amount of elastic strain energy is stored within them during folding. Care must be exercised to ensure that this energy is released in a controlled fashion during deployment. When deployment is complete the shell recovers its unstrained, extended configurations (S. Pellegrino, 2001). STEMs have found use on spacecraft as antennas, booms to carry instruments, and booms to serve to increase the spacecraft's inertia moments, as docking booms, as grapping devices, as elements for the extension and support of large ligh-weight space structures; STEM-like structures, whose cross-section is that of a partial tube, i.e. characterised by an embrace angle of less than 180°, are finding use ah hinges.

We are considering the use of shape memory alloy wires embedded into the fabric in order to trigger the bi-stable configuration changes and, at the same time, increasing the efficiency of

the process (in terms of repetitivity and speed) and optimising the extended configuration (e.g. radius of curvature, overlap length, thickness to radius ratio). The deployable bi-stable tubes are stable in the straight and strain-free configuration as well as in the second coiled configuration where they are subjected to high strain (in elastic condition) but they are unable to jump towards a zero-energy state, because the rolled up configuration corresponds to a local minimum of the potential energy surface. The key to their bi-stable behaviour is the particular composite construction, in which the fibres are arranged at $\pm\alpha$ to the longitudinal axis using an antisymmetric construction[2].

The main issues related to such concept comprise:

- activation of SMA fibres embedded in the composite structure through temperature by solar radiation;
- prediction of the performance of the structure from the combination of the main parameters (stacking sequence, thermoplastic resin properties, fibre material, SMA fibres density, etc.);
- demonstration by manufacturing of thin walled composite structures with embedded SMA wires along $\pm\alpha$ directions (Figure 14);
- exploitation of centrifugal force in order to activate deployment, in combination with the action of SMA wires;
- pre-straining of the tubular structure by using SMA fibres (which have to be localised away from the neutral axis to contribute most to the second moment of area).

For the proposed case study the key idea is the integration of SMA into a thermo-plastic composite to allow a bistable behavior "from rolled to tubular" in response to heating, for instance caused by solar radiation (Figure 15). That will demonstrate that it is possible to pack the structure into a volume many times smaller (high packing efficiency) than its

[2] Antisymmetric laminate implies that the material of layers above the laminate midplane are identical to those below, but the orientations are of opposite sign.

deployed volume, without damaging the structural integrity. Applicability of this technology to various classes of devices is evident: compact carriage, reduced masses and launch costs.

The main phases of the project comprise:

- SMA wire selection (material, wire diameter, wires density and configuration);
- thermoplastic material selection;
- modeling of SMA wire – polymer composite behavior.

Different configurations of booms could be considered as depicted into the Figure 16.

The choice of overlap in STEMs depends upon several factors and the angle subtening the overlap ranges from 155 to 167. STEMs are produced by forcing a flat tape into a tubular form, and then heat treating it such that it retains its tubular shape. In this case, the structure is not really bi-stable and the tube in the coiled configuration will jump to the straight configuration in absence of a deployable activating mechanism.

Different material properties and combination of materials can be considered. Two "antagonistic" solutions comprise the use of thermosetting resin systems and thermoplastic reinforced with unidirectional carbon fibres. In one case a Cyanamid Fothergill GY-70 unidirectional carbon HM is considered (ESA, Composite Design Handbook). In the second case a continuous fiber reinforced thermoplastic with unidirectional E-glass fiber reinforcement and polypropylene resin, is considered. Properties of glass/PP unidirectional and T300/2500 composites are reported in Table 1.

Considering the above material properties, and a boom with a wall thickness of about 1.0 millimetres, 4 plies need to be considered using glass/PP and 16 layers using carbon/epoxy. In the first case possible stacking sequences are ($\pm\alpha/\pm\alpha$) or ($+\alpha/0/90/-\alpha$), being α equal to 30, 45 or 60 degrees. In the second case ($\pm\alpha/0/\pm\alpha/90/\pm\alpha/\pm\alpha/0/\pm\alpha/90/\pm\alpha$), or ($\pm\alpha/0_2/\pm\alpha/0_2/90_2/\pm\alpha/90_2/\pm\alpha$), α equal to 30, 45 or 60 degrees. In both cases the laminate

set-up is made up of a combination of 0°/90° and ± α ° layers. In addition to a favourable influence on the buckling behaviour of the very thin-walled structure, the choice of the stacking sequence is essentially based on the requirement to minimize the bending that takes place during single-sided thermal loading as it will be expected if the booms are exposed to the radiation environment in space. For this reason, a very low coefficient of thermal expansion (CTE) in the boom longitudinal direction is an important prerequisite (CTE ≈ 0 K^{-1}). The demand for an ultra-light Gossamer structure inevitably leads to a membrane-like, thin-walled structure that has an extremely large surface in relation to its volume and, as a result, has an intensive exchange of radiation with its environment. Minimum and maximum temperatures, thermal gradients in the boom cross-section, and transient events such as the shadowing of sub-systems or the Earth eclipse therefore have to be particularly taken into consideration during the boom design and material selection process.

Because of the role it plays in the entire concept, the structural design of the booms is very significant. Stiffness restrictions, such as those in the form of minimum bending stiffness requirements, as well as strength requirements are usually defined. From a global point of view, the booms can be described by defining the beam stiffness EI_x, EI_y, GJ_z and EA with an uniaxial beam model. The loading limit, on the other hand, is characterized in the thin-walled profile only by the buckling stability that, as an essential part of the structural description, has to be analyzed in detail. The axial booms must be sufficiently rigid to avoid elastic instability and subsequent collapse.

The computation of the snap-through buckling behaviour of a shell structure is rather complex due to its non-linear character and can be done analytically in only a few cases.

Highly nonlinear Finite Element (FE) computations are applied to the analysis of the boom stability behaviour.

Some preliminary analyses have been performed with the program ANSYS. Using the program ANSYS it is possible to perform nonlinear buckling analysis, which employs a

nonlinear static analysis with gradually increasing loads to seek the load level at which the structure becomes unstable. Using the nonlinear technique, the model can include features such as initial imperfections, plastic behaviour, gaps, and large-deflection response. In addition, using deflection-controlled loading, it is possible to track the post-buckled performance of the structure (which can be useful in cases where the structure buckles into a stable configuration, such as "snap-through" buckling of a shallow dome).

If the loading on the structure is perfectly in-plane (that is, membrane or axial stresses only), the out-of-plane deflections necessary to initiate buckling will not develop, and the analysis will fail to predict buckling behaviour. To overcome this problem, it is required to apply a small out-of-plane perturbation, such as a modest temporary force or specified displacement, to begin the buckling response. A preliminary eigenvalue buckling analysis of the structure may be useful as a predictor of the buckling mode shape, allowing to choose appropriate locations for applying perturbations to stimulate the desired buckling response. The imperfection (perturbation) induced should match the location and size of that in the real structure. The failure load is very sensitive to these parameters.

The composite structure has been modelled using element types shell 99 of the ANSYS library, a layered shell element with six degrees of freedom at each node. The element allows to input the stacking sequence in matrix form through the definition of the three stiffness matrices, A, B and D membrane, membrane-bending coupling and bending stiffness matrix, respectively. The membrane stiffness matrix, A, relates the in-plane stress resultants N to the mid-surface strains, and the bending stiffness matrix, D, relates the stress couples M to the curvatures, κ. Since the B matrix relates the stress couples M do the strains and the stress resultants N to κ, it is called the membrane-bending coupling matrix. The above matrices can be calculated for a laminate as follows (ESA PSS-03-1101, 1986):

$$A = \sum_{k=1}^{N} \overline{Q}_k \cdot \left(h_k - h_{k-1}\right)$$

$$B = \frac{1}{2} \sum_{k=1}^{N} \overline{Q}_k \cdot \left(h^2{}_k - h^2{}_{k-1}\right)$$

$$D = \frac{1}{3} \sum_{k=1}^{N} \overline{Q}_k \cdot \left(h^3{}_k - h^3{}_{k-1}\right)$$

where h_i defines the distance of the ply interfaces of the i-th layer from the midplane and $\overline{Q}_k$ is the stiffness matrix, relating stress and strain in (1,2) coordinates for i-th layer.

From material properties provided in Table 1, and considering a thermoset composite structure composed by 16 layers with orientation ($\pm 45/0/\pm 45/90/\pm 45$ $/\pm 45/0/\pm 45/90/\pm 45$) (total thickness 0.96 millimetres), the following stiffness matrices A, B, and D have been calculated:

$$A = \begin{pmatrix} 156.88 & 72.946 & 0 \\ 72.946 & 156.88 & 0 \\ 0 & 0 & 56.246 \end{pmatrix} \text{GPa} \cdot \text{mm}$$

$$B = \begin{pmatrix} -2.962 & 0 & -2.962 \\ 0 & 2.962 & -2.962 \\ -1.481 & -1.481 & 0 \end{pmatrix} \text{GPa} \cdot \text{mm}^2$$

$$D = \begin{pmatrix} 12.123 & 5.527 & 0 \\ 5.527 & 12.123 & 0 \\ 0 & 0 & 4.17 \end{pmatrix} \text{GPa} \cdot \text{mm}^3$$

Considering a thermoplastic composite composed by 4 layers with orientation ($\pm 45/\pm 45$) (total thickness 1.0 millimetres), the following stiffness matrices have been obtained:

$$A = \begin{pmatrix} 17.669 & 8.169 & 0 \\ 8.169 & 17.669 & 0 \\ 0 & 0 & 4.212 \end{pmatrix} \text{GPa} \cdot \text{mm}$$

$$B = \begin{pmatrix} 0 & 0 & -1.501 \\ 0 & 0 & -1.501 \\ -0.75 & -0.75 & 0 \end{pmatrix} \text{GPa} \cdot \text{mm}^2$$

$$D = \begin{pmatrix} 1.472 & 0.681 & 0 \\ 0.681 & 1.472 & 0 \\ 0 & 0 & 0.351 \end{pmatrix} \text{GPa} \cdot \text{mm}^3$$

The model representing a boom configuration corresponding to a closed tube (see configuration a of Figure 16) is shown in Figure 17a. The model is composed by 4,050 shell elements representing the composite structure of the boom and by 211 shell elements representing the top of the boom where a bulkhead has been included. The bulkhead has the scope of avoiding local instability of the top of the structure where an axial load has been imposed, equal to 500 N. Figure 18 shows a particular of the model where an imperfection has been simulated by reducing the stiffness properties of eight elements. The introduction of an imperfection is required to initiate the nonlinear solution. In this case the first eigenform is analysed.

The results of the simulation considering the thermoset material are shown in figures from Figure 19 to Figure 23. Figure 19 shows the deformed shape of the structure. Figure 20, Figure 21 and Figure 22 show the distribution of the displacements along the x, y and the z directions, respectively. Figure 23 shows the distribution of the total displacements. The value of the critical buckling load calculated is equal to 153 kN. The results of the simulation considering the thermoplastic material are shown in figures from Figure 24 to Figure 28. Figure 24 shows the deformed shape of the structure. Figure 25, Figure 26 and Figure 27 show the distribution of the displacements along the x, y and the z directions, respectively.

Figure 28 shows the distribution of the total displacements. The value of the critical buckling load calculated is equal to 17.8 kN.

A second finite element model has been prepared representing a boom configuration corresponding to an open bistable tube (see configuration c of Figure 16). The model is shown in Figure 17b. The model is composed by 4,200 shell elements modelling the composite structure of the boom and by 274 shell elements modelling the top bulkhead. The results of the simulation considering the thermoset materials are shown in figures from Figure 29 to Figure 33. The value of the critical buckling load calculated is equal to 55.7 kN. The results of the simulation considering the thermoplastic materials are shown from Figure 34 to Figure 38. The value of the critical buckling load calculated is equal to 3.46 kN.

3 CONCLUSIONS

The work performed in the framework of the Bionics and Space System Design has lead to the identification of four case studies which have been analyzed and described in the previous chapters. Based on the different and complementary expertise of the Biomimicry Expert Group, D'Appolonia has assigned each of the case studies selected by ESA to a different working team. In order to facilitate the management activities, a responsible has then been selected within each working group. The work has lead to a better understanding of the biological principle, together with a first attempt of an engineering solution.

Within the test case related to the "Energy Storage Structures for Deployable Systems", the biological principle studied is the mechanism of rapid closure of the leaf of the Venus Fly Trap. This mechanism inspired a new concept of deployable booms for space applications (antennas and solar reflectors) made in thermoplastic composite material. The suitability of the concept is demonstrated though buckling analysis of several configurations characterised by different laminated stacking sequences and fibre orientations. Further steps for the development of the concept would comprise the study of incorporation of SMA elements into the composite structures for the control of the bistable structure.

RDL/DMZ/SMC/AB:ad

REFERENCES

Ashida, J., 1934, "Studies on the leaf movement of Aldrovanda vesiculosa", L. I Process and mechanism of movement. Memories of the College of Science, Kyoto Imperial University, Ser B 9, 14-184

Darwin, C., 1875, Insectivorous Plants, London

DLR: Philae Lander Fact Sheets, http://www.dlr.de/DLRRosetta/ background/Philae_Lander_FactSheets.pdf, 2004.

Forterre Y., J.M. Skotheim, J. Dumais, L. Mahadevan, 2005, "How the Venus flytrap snaps", Nature, Vol. 433, January, 421-425

Hodick D., A. Sievers, 1989, "On the mechanism of trap closure of venus flytrap Dionaea muscipula", Planta, vol. 179, 32-42

Jeronimidis G., A.T. Parkyn, 1988, "Residual stresses in carbon fibre thermoplastic matrix laminates", Journal of Composite Materials, vol. 22, 401-415

Lagoudas, D.C., I.G. Tadjbakhsh, 1992,"Active flexible rods with embedded SMA fibers", Smart Mat. And Struct., Vol.1, pp. 162-167)

NASA, "Critical Requirements for the design of large space structures", 1981.

Otsuka K. and C. M. Wayman, 1998, "Shape Memory Materials", Cambridge University Press, Cambridge, CB2 2RU, UK

Pellegrino, S., 2001, Deployable Structures, CISM International Centre for Mechanical Sciences. Courses and Lectures, No. 412

Rogers C., C. Liang, J. Jia, 1989, "Behavior of shape memory alloy reinforced composites. Part I: Model formulations and control concepts", Proc., 30th Struct., Struct. Dyn. And Mat. Conf., Paper No. AIAA 89-1389-CP, pp. 2011-2017

Sickinger C., L. Herbeck, T. Strohlein, J. Torres-Torres, 2004, "Lightweight Deployable booms: Design, Manufacture, Verification and Smart materials applications", IAC-04-1.4.10

von Guttenberg H., 1959, "Die physiologische anatomie seismonastisch reaktionsfähiger Organe", Handbuch der Pflantzenphysiologie, Springer, pp. 175-191

von Guttenberg H., 1971, "Bewegungsgewebeund Perzeptionsorgane", Handbuch der Plantzenanatomie, Verlag Gebr., pp. 171-175

Williams S.E., A.B. Bennet, 1982, „Leaf Closure in the Venus Flytrap: an aciid growth Response", Science, Vol. 218, 1120-1122

TABLE 1
PROPERTIES OF GLASS/PP UNIDIRECTIONAL AND T300/2500 COMPOSITES

	glass/PP	carbon/epoxy
Young's modulus along the fibres (GPa)	26.6	275
Young's modulus perpendicular to the fibres (GPa)	2.97	4.6
Shear Modulus in 1-2 plane (GPa)	1.39	2.7
Major Poisson's ratio	0.4	0.35
Minor Poisson's ratio	0.04	*0.04*
Specific weight (gr/cm^3)	1.64	1.6
Ply thickness (mm)	0.25	0.06

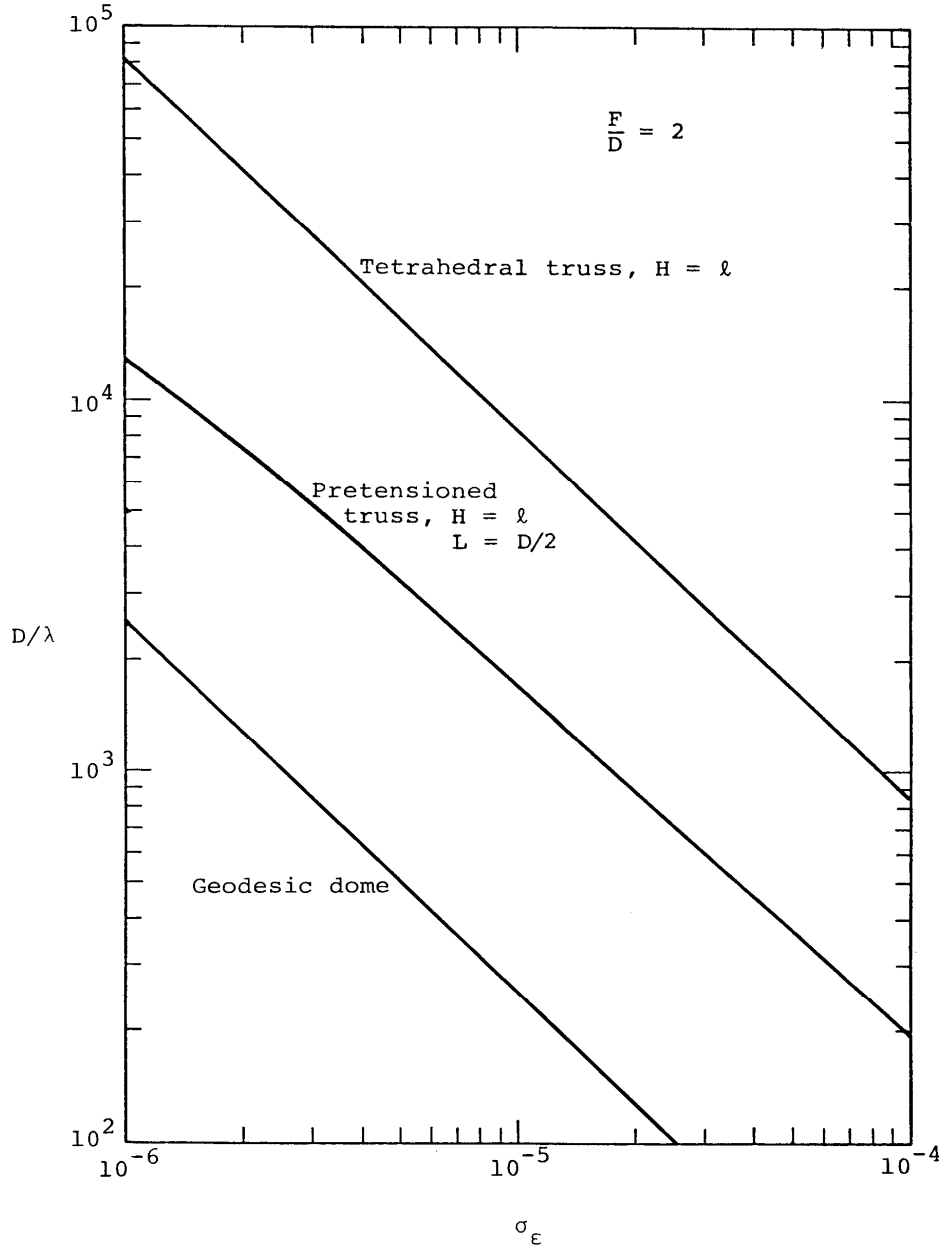

FIGURE 1

POTENTIAL ANTENNA SIZES FOR WRMS= Λ/100 AS LIMITED BY FABRICATION IMPERFECTIONS

PREPARED FOR

ESA, ESTEC
Noordwijk, The Netherlands

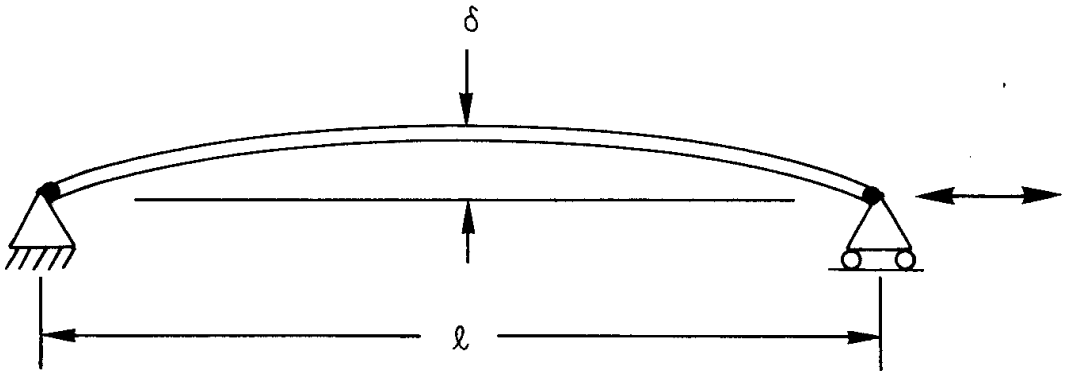

$$\frac{EA_{eff}}{EA} = \frac{1}{1 + \frac{1}{2}\left(\frac{\delta}{k_c}\right)^2} \quad , \quad k_c = \sqrt{\frac{I}{A}}$$

FIGURE 2

EFFECT OF OUT-OF-STRAIGHTNESS ON AXIAL STIFFNESS

PREPARED FOR

ESA, ESTEC
Noordwijk, The Netherlands

ℓ/k_c <	CASE
$\frac{573.9}{\ell^{1/3}}$	Horizontal testing. Gravity sag < $k_c/3$
$\frac{2700}{\ell^{1/2}}$	Vertical testing. Tension < 1/10 Euler load
1633	Fabrication. $\Delta\varepsilon = 10^{-6}$
414	Built-in loads < 1/10 Euler load, $\sigma_\varepsilon = 10^{-5}$
$2.8\ \frac{D^2}{H\ell}$	Member vibration frequency > 3 truss frequency, $m_p/m_2 = 2$, $k = 2$

FIGURE 3

ALLOWABLE MEMBER SLENDERNESS. LENGTH L IS IN METERS. MEMBER DENSITY = 1520 kg/m3; YOUNG'S MODULUS = 110 GPa

PREPARED FOR

ESA, ESTEC
Noordwijk, The Netherlands

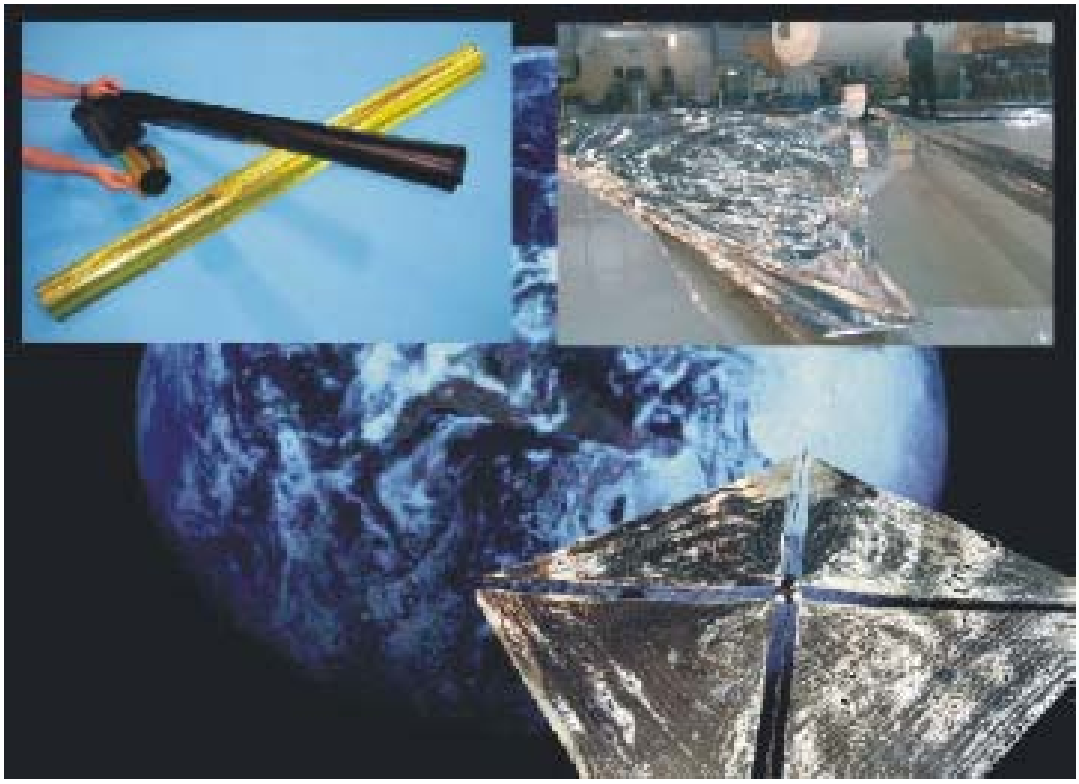

FIGURE 4

SOLAR SAIL PHASE 1 – EARTH ORBIT DEPLOYMENT DEMONSTRATION: ESA AND DLR ARE PLANNING THE DEMONSTRATION IN A JOINT EFFORT. THE DLR INSTITUTE OF STRUCTURAL MECHANICS IS INVOLVED BY THE HARDWARE CONTRIBUTION OF DEPLOYABLE CFRP BOOMS AND ULTRA-THIN SAIL SEGMENTS. [COURTESY OF DLR].

PREPARED FOR

ESA, ESTEC
Noordwijk, The Netherlands

FIGURE 5

DEPLOYABLE CFRP BOOM. LENGTH 14 m,
MASS 1.4 kg [COURTESY OF DLR]

PREPARED FOR

ESA, ESTEC
Noordwijk, The Netherlands

FIGURE 6

THE INTERNAL DEFORMATION ENERGY OF A STOWED BOOM PACKAGE ENABLES THE SELF-DEPLOYMENT OF THE 14m IONG BOOM [COURTESY OF DLR].

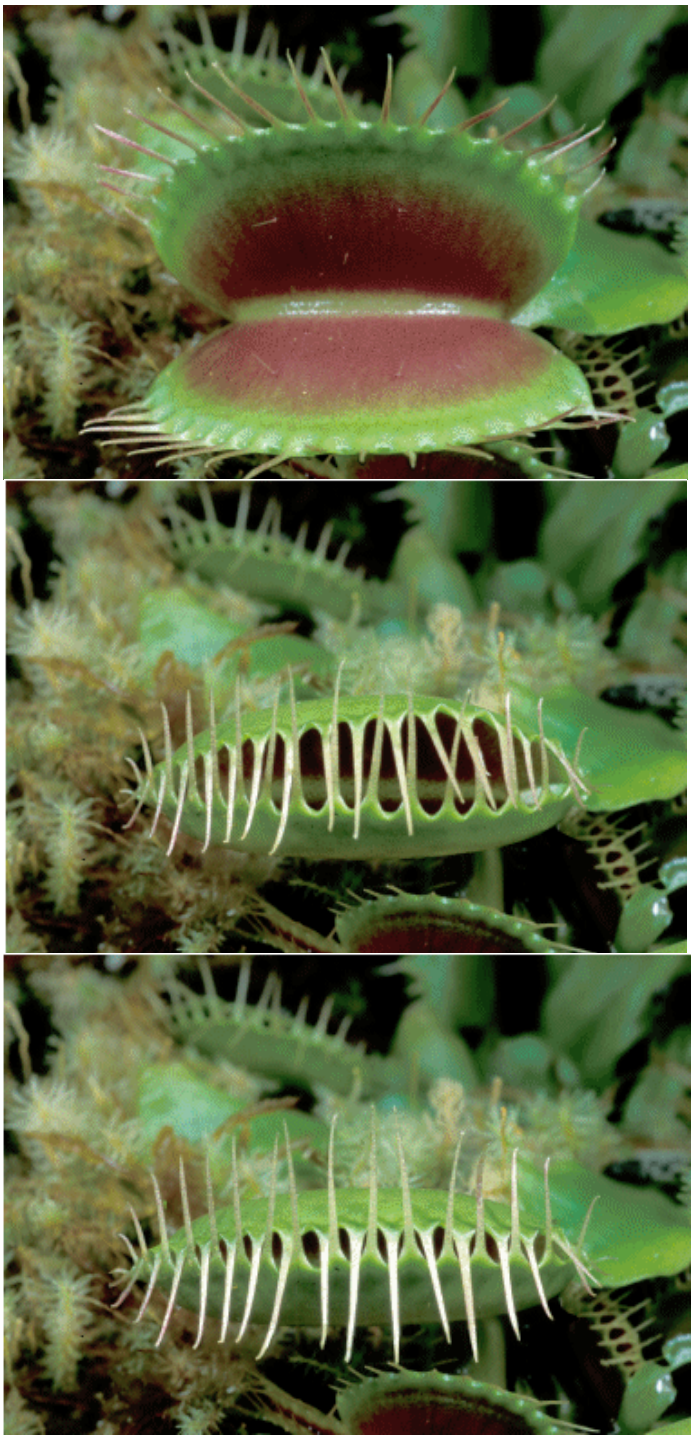

(Reference: http://www.sarracenia.com/galleria/g311.html)

FIGURE 7

CLOSURE OF VENUS
FLYTRAP LEAF

PREPARED FOR

ESA, ESTEC
Noordwijk, The Netherlands

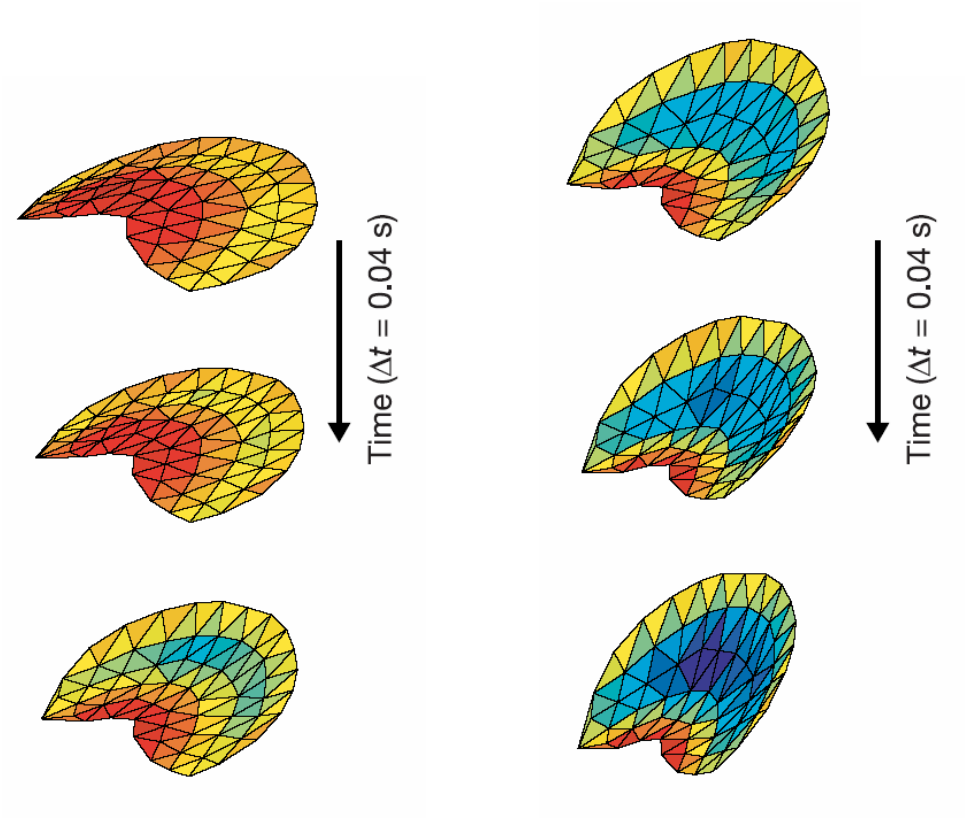

FIGURE 8

DYNAMIC SEQUENCE OF THE LEAF CLOSURE (FROM FORTERRE ET AL., 2005)

PREPARED FOR

ESA, ESTEC
Noordwijk, The Netherlands

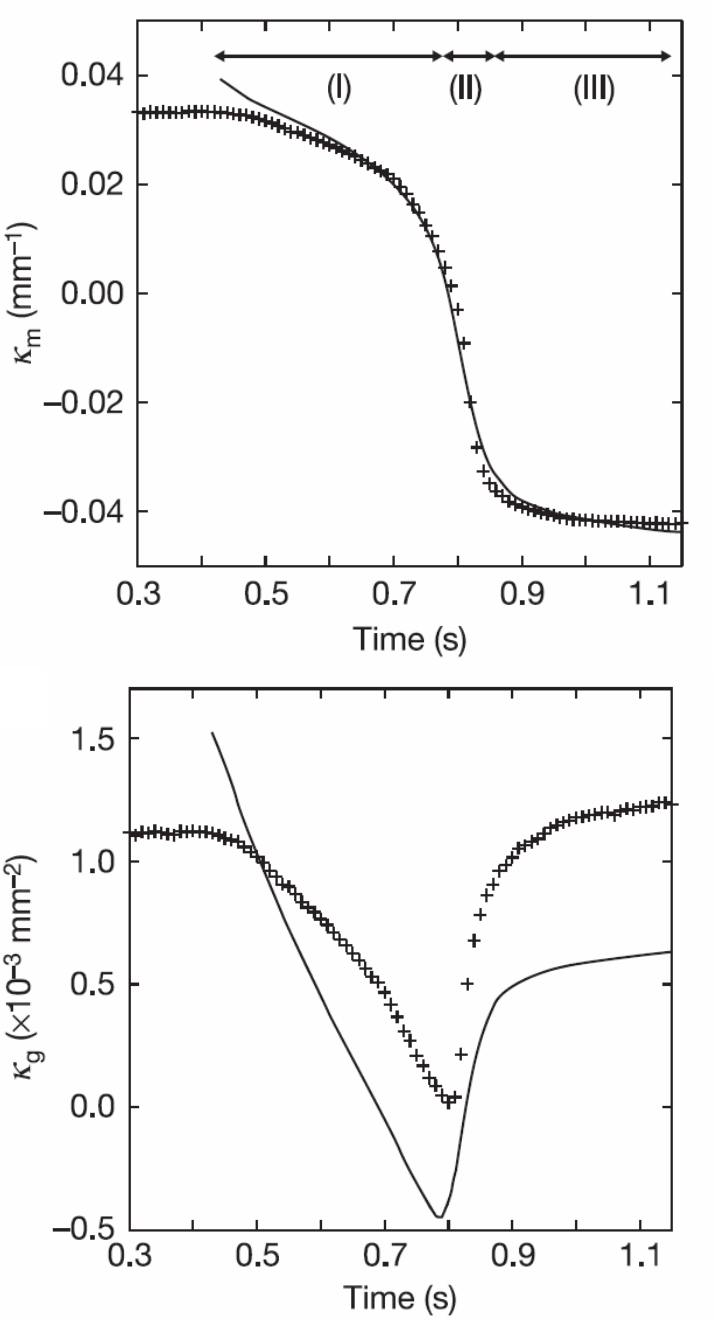

FIGURE 9

SPATIALLY AVERAGED MEAN CURVATURE k_m AND GAUSSIAN CURVATURE K_G AS A FUNCTION OF TIME

PREPARED FOR

ESA, ESTEC
Noordwijk, The Netherlands

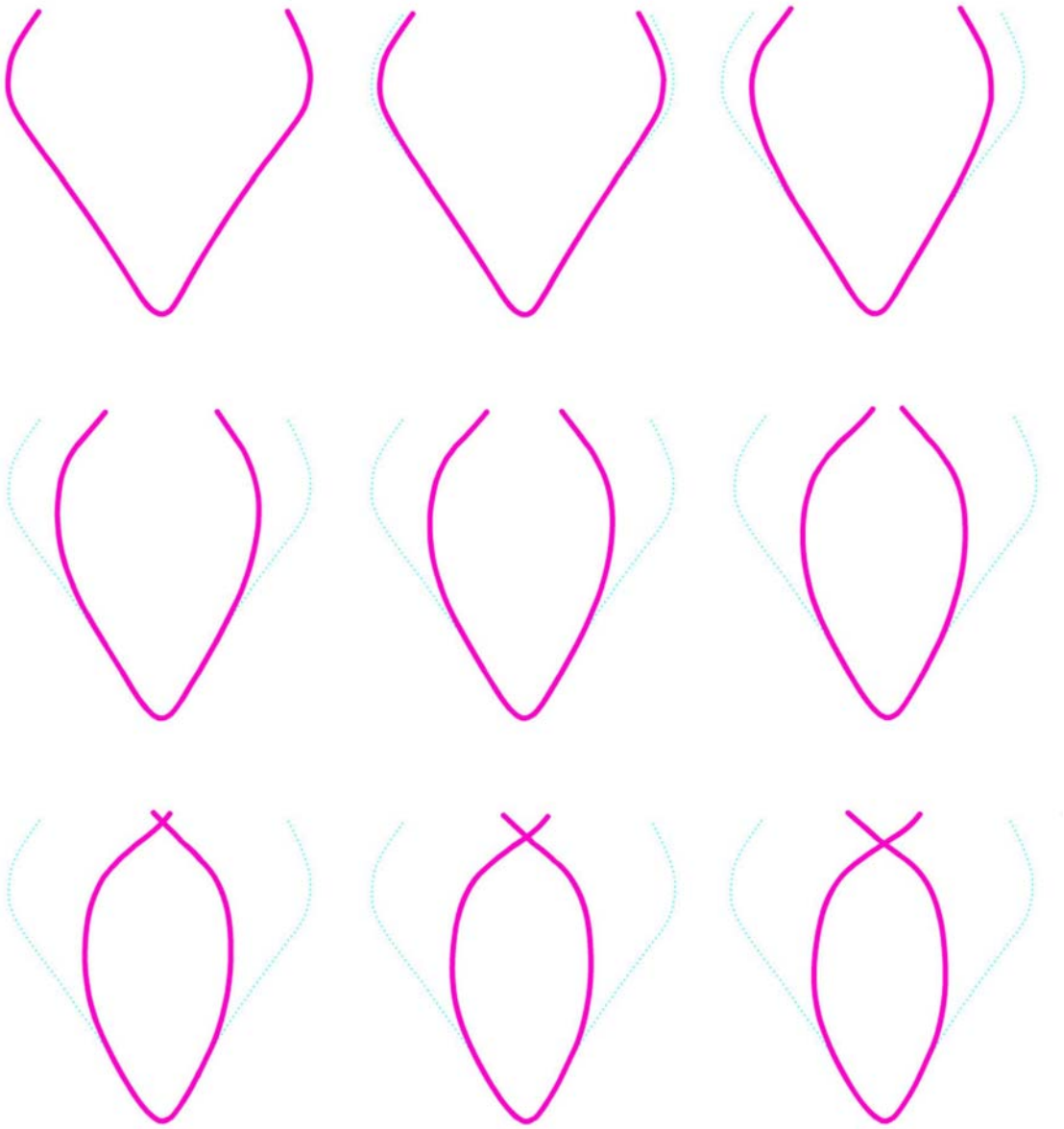

FIGURE 10

SEQUENCE OF LEAF CLOSURE

PREPARED FOR

ESA, ESTEC
Noordwijk, The Netherlands

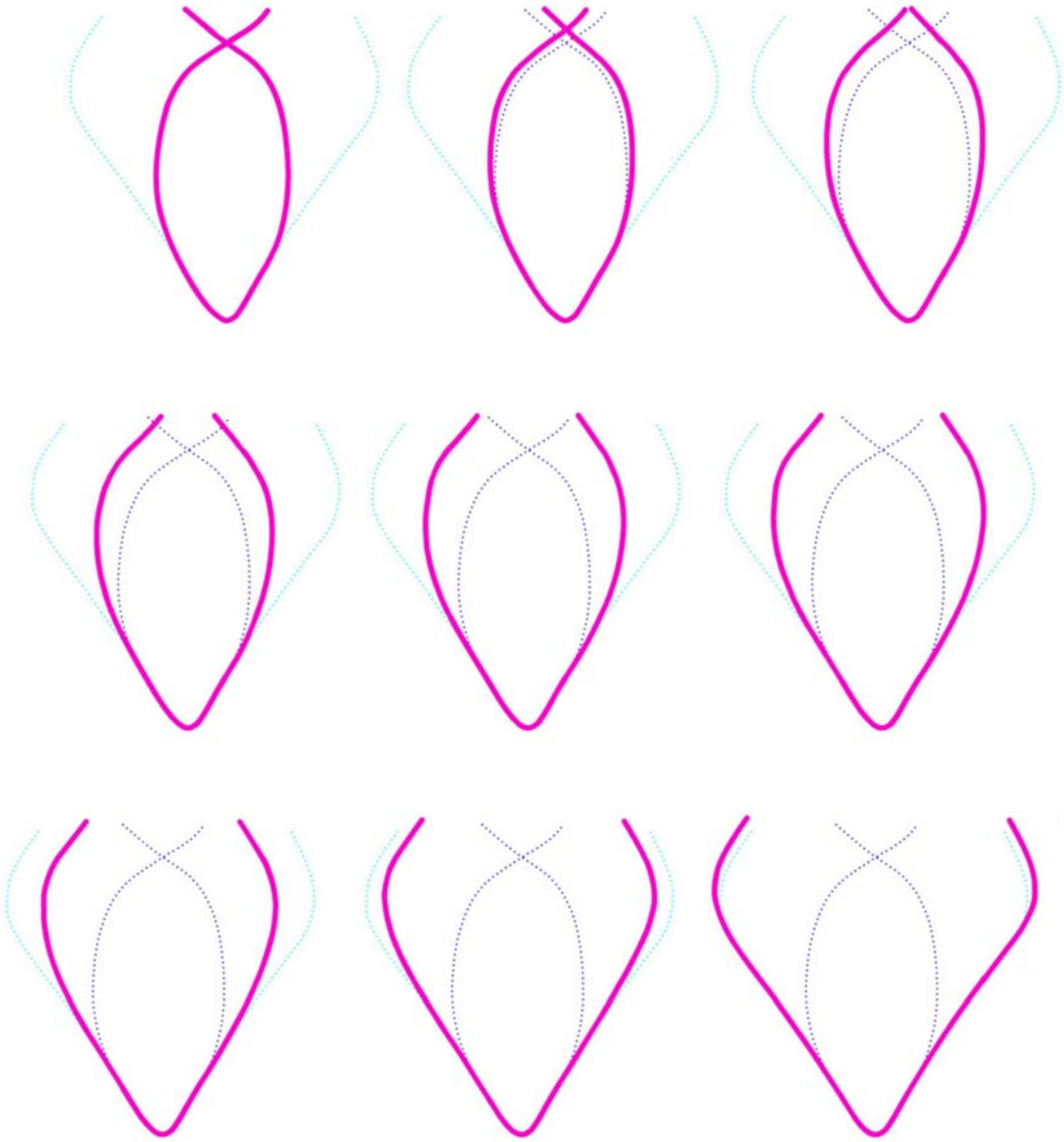

FIGURE 11

SEQUENCE OF LEAF OPENING

PREPARED FOR

ESA, ESTEC
Noordwijk, The Netherlands

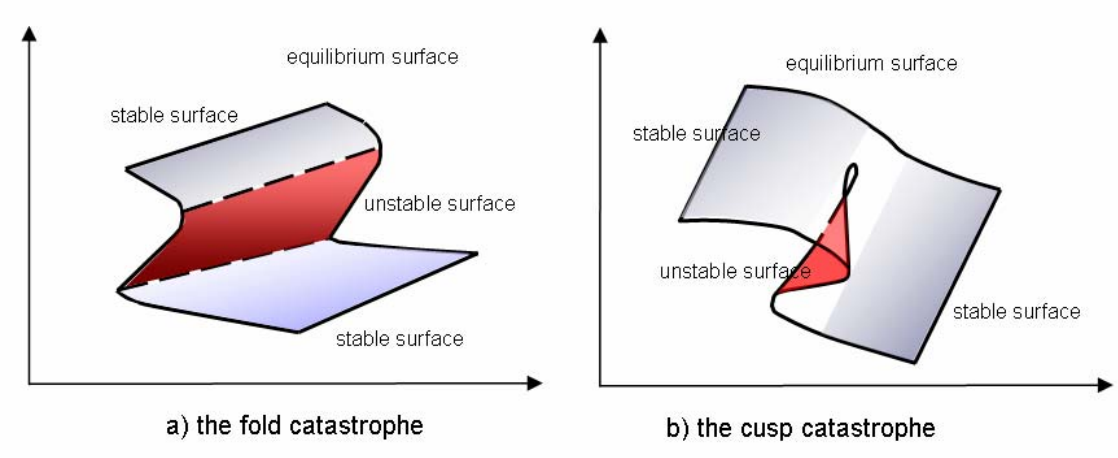

FIGURE 12

CUSP AND FOLD SHAPES OF THE CATASTROPHE THEORY

PREPARED FOR

ESA, ESTEC
Noordwijk, The Netherlands

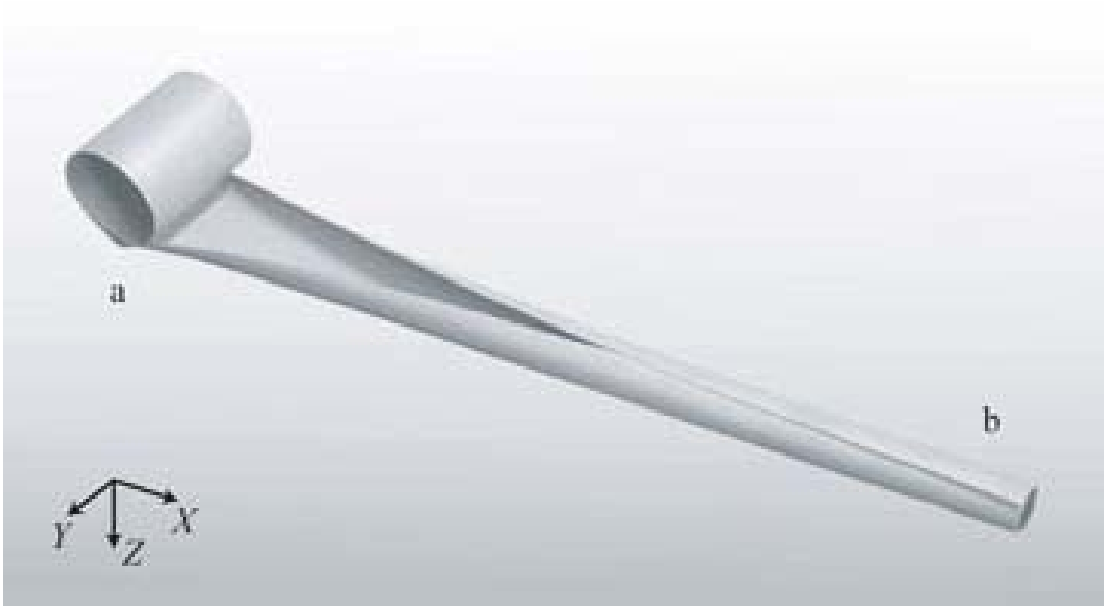

FIGURE 13

WINDING MECHANISM OF BISTABLE TUBE

PREPARED FOR

ESA, ESTEC
Noordwijk, The Netherlands

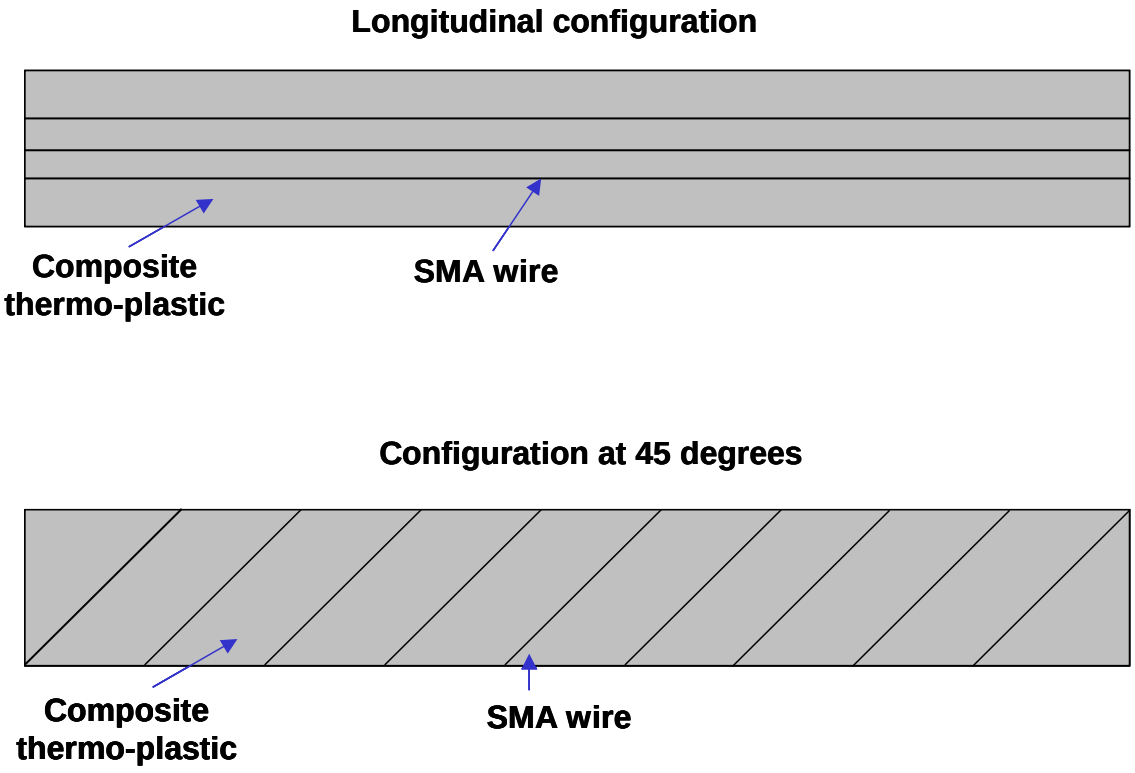

FIGURE 14

SMA ELEMENTS EMBEDDED INTO A LAMINATE WITH DIFFERENT ORIENTATIONS (0° AND 45°) THE OPERATING PRINCIPLE IS DEPICTED IN THE FOLLOWING FIGURE.

PREPARED FOR

ESA, ESTEC
Noordwijk, The Netherlands

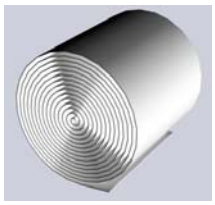

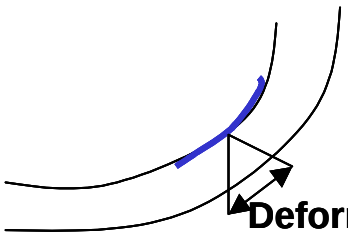

Martensite state

Heating

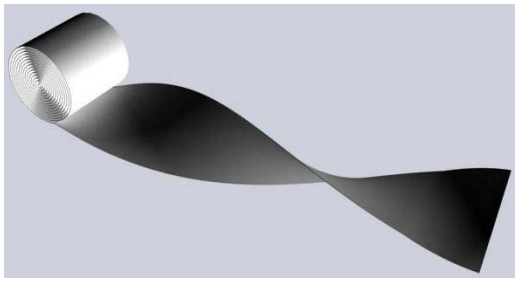

Austenite state

FIGURE 15

TWIST IN SMA HYBRIDISED FIBRE
THERMOPLASTIC MATRIX LAMINATE

PREPARED FOR

ESA, ESTEC
Noordwijk, The Netherlands

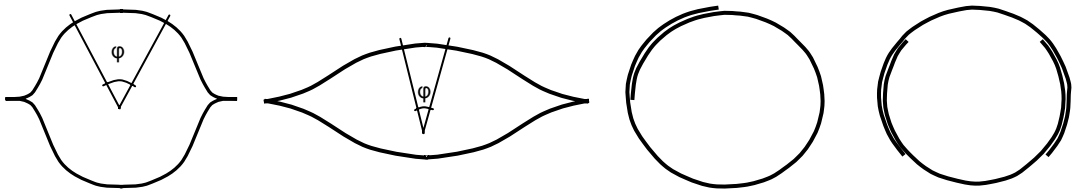

a) collapsible closed tube; φ = 60° b) collapsible closed tube; φ = 30° c) STEM d) bi-STEM

FIGURE 16

BOOMS CONFIGURATIONS

PREPARED FOR

ESA, ESTEC
Noordwijk, The Netherlands

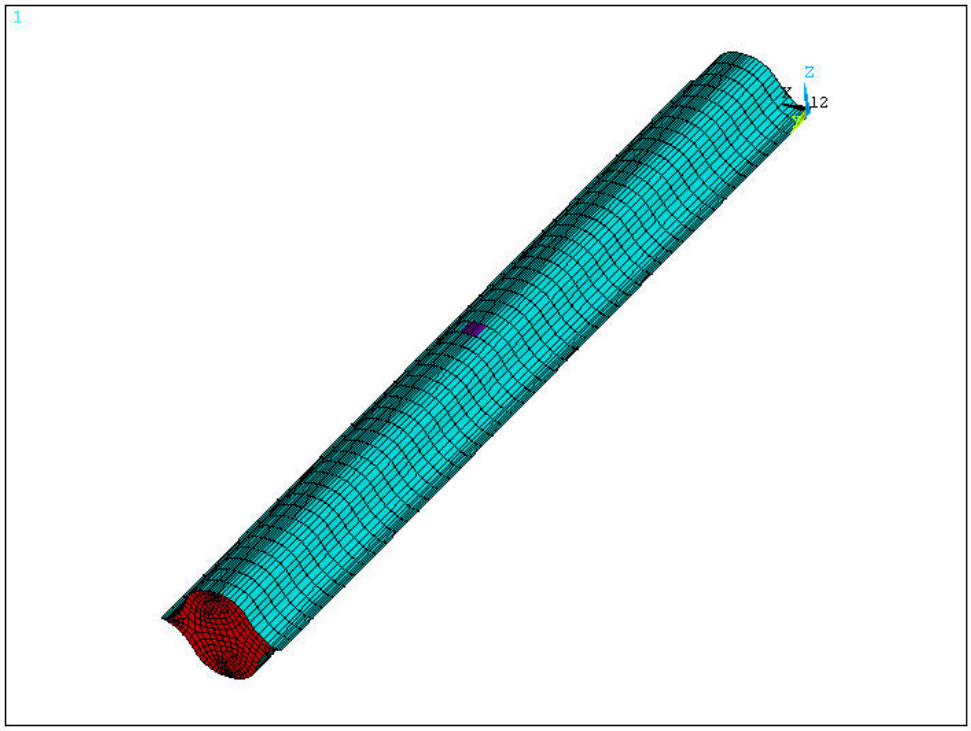

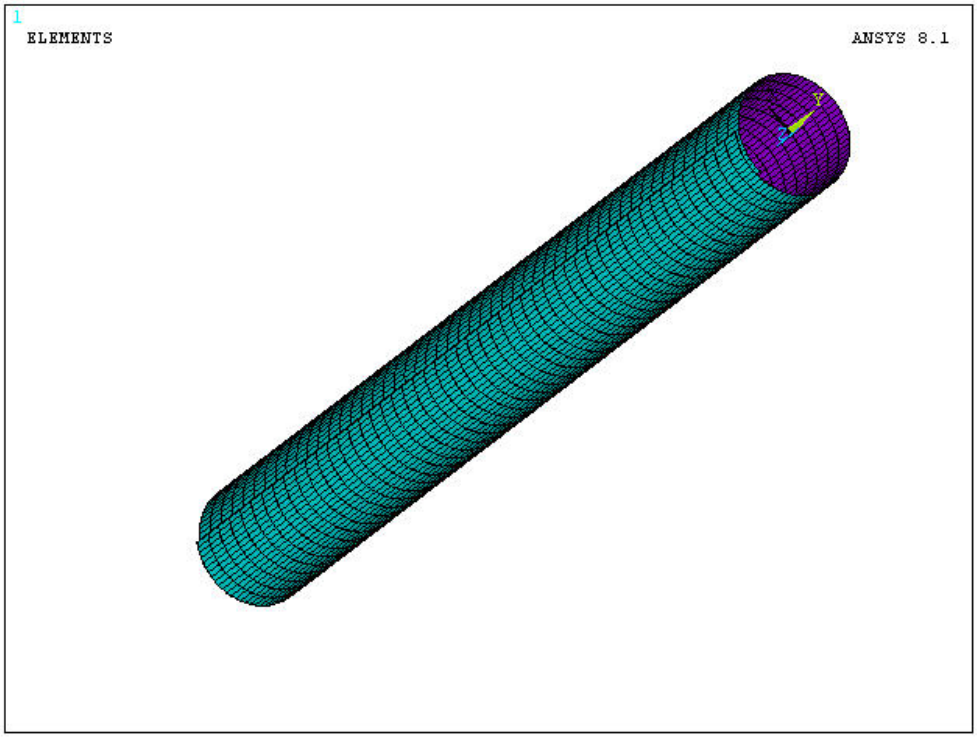

FIGURE 17

FEM MODEL OF DEPLOYABLE BOOM
CLOSED SECTION (A)
AND OPEN SECTION (B)

PREPARED FOR

ESA, ESTEC
Noordwijk, The Netherlands

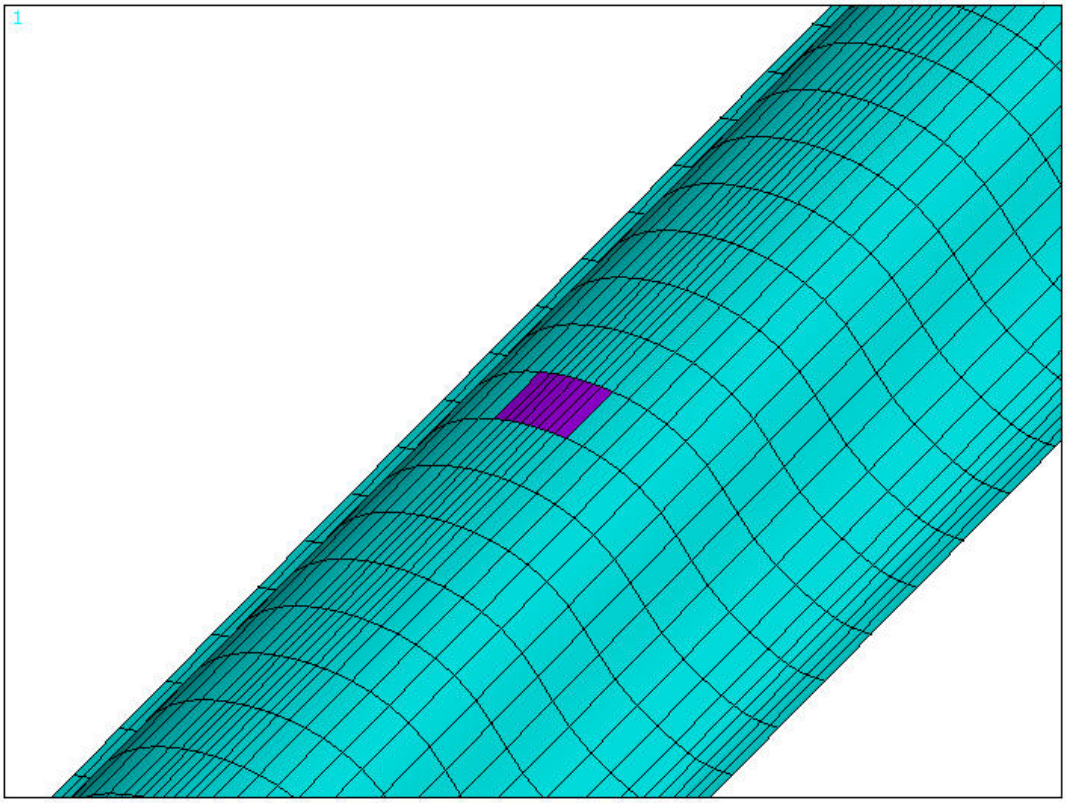

FIGURE 18

PARTICULAR OF FEM MODEL OF DEPLOYABLE BOOM WITH IMPERFECTION SIMULATED AS ELEMENTS CHARACTERISED BY REDUCED MATERIAL PROPERTIES

PREPARED FOR

ESA, ESTEC
Noordwijk, The Netherlands

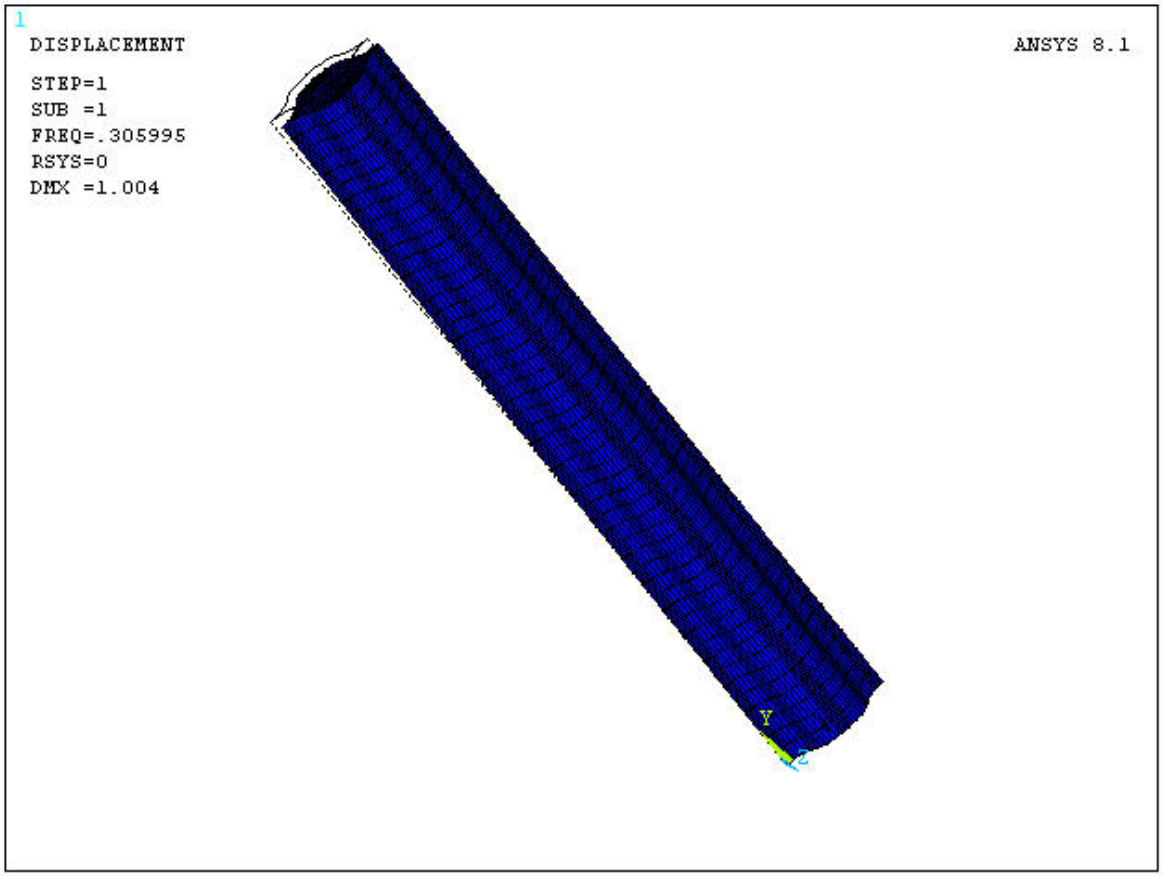

FIGURE 19

DEFORMED STRUCTURE OF
THERMOSETTING COMPOSITE BOOM
(CLOSED SECTION).

PREPARED FOR

ESA, ESTEC
Noordwijk, The Netherlands

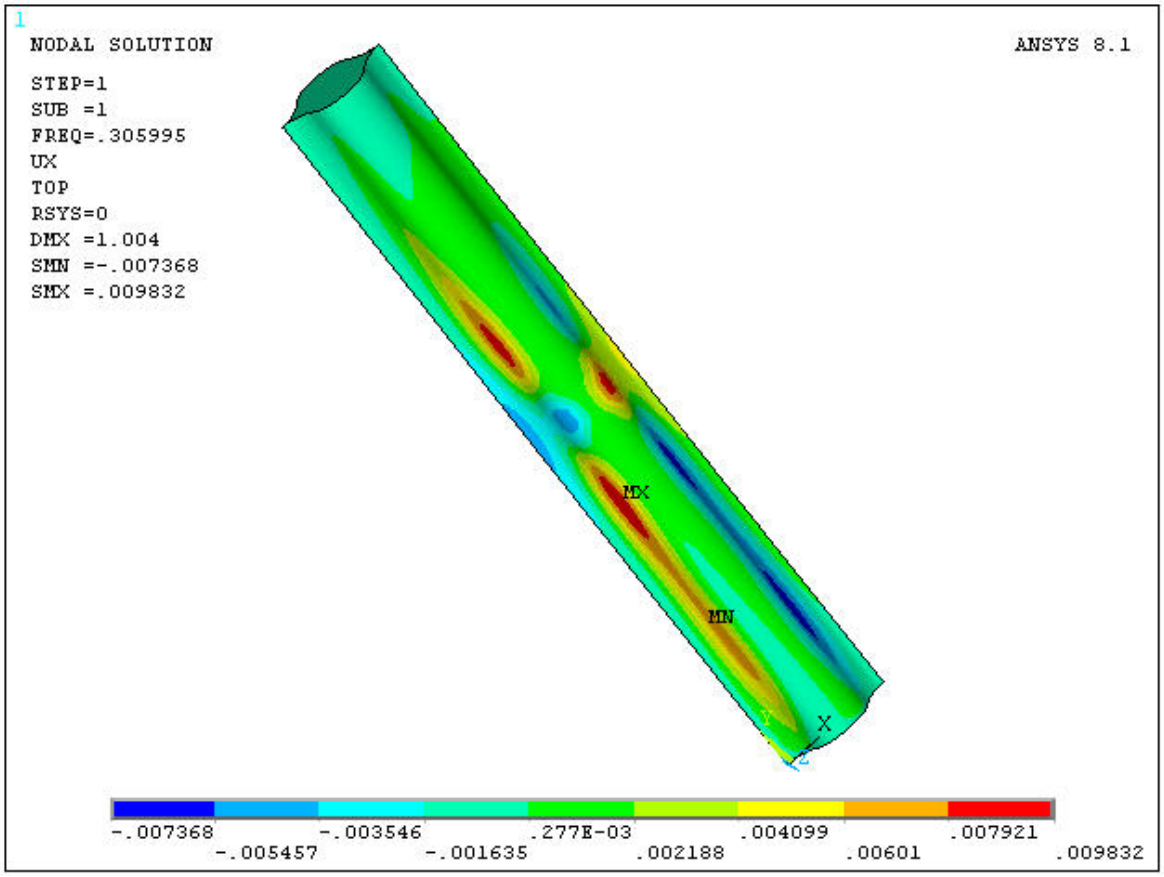

FIGURE 20

DISPLACEMENTS (MILLIMETRES) ALONG DIRECTION X OF THERMOSETTING DEPLOYABLE BOOM (CLOSED SECTION).

PREPARED FOR

ESA, ESTEC
Noordwijk, The Netherlands

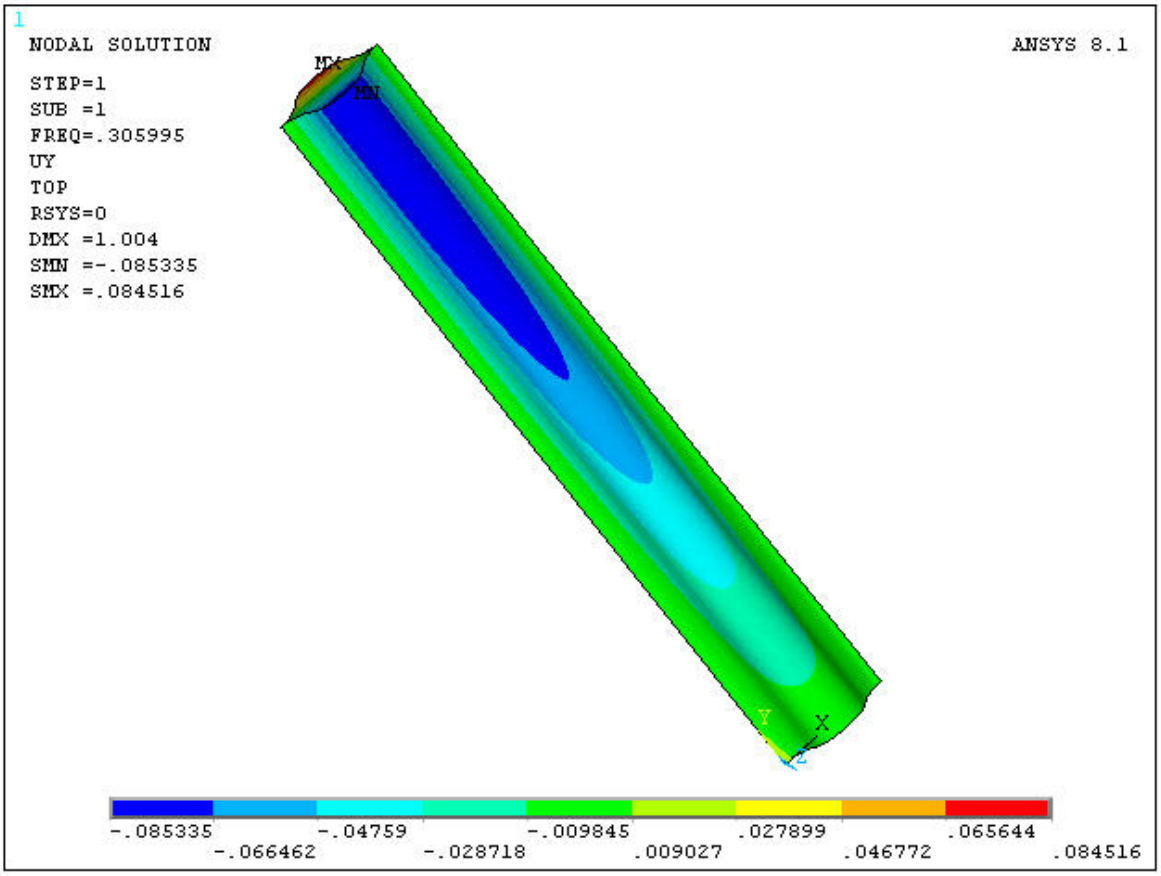

FIGURE 21

DISPLACEMENTS ALONG Y (MILLIMETRES) OF THERMOSETTING DEPLOYABLE BOOM (CLOSED SECTION).

PREPARED FOR

ESA, ESTEC
Noordwijk, The Netherlands

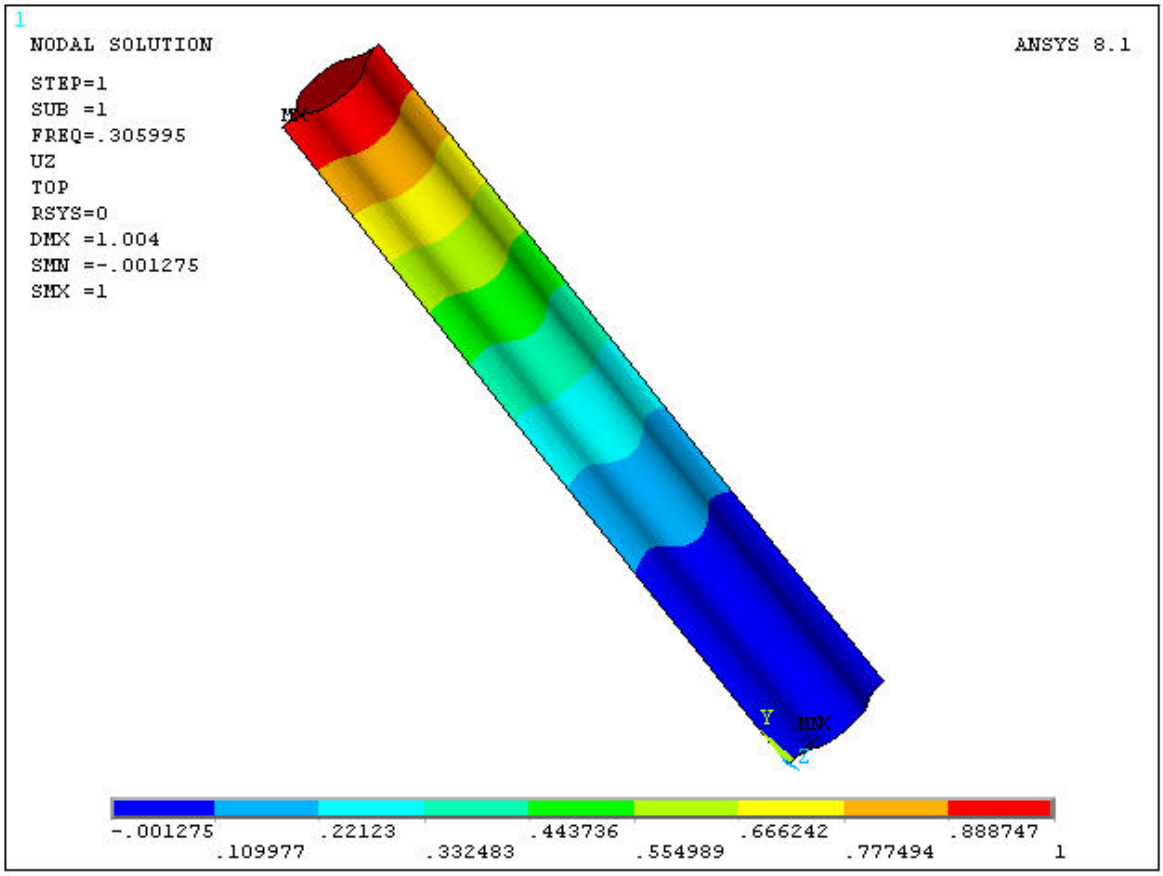

FIGURE 22

DISPLACEMENTS ALONG Z (MILLIMETRES) OF THERMOSETTING DEPLOYABLE BOOM (CLOSED SECTION).

PREPARED FOR

ESA, ESTEC
Noordwijk, The Netherlands

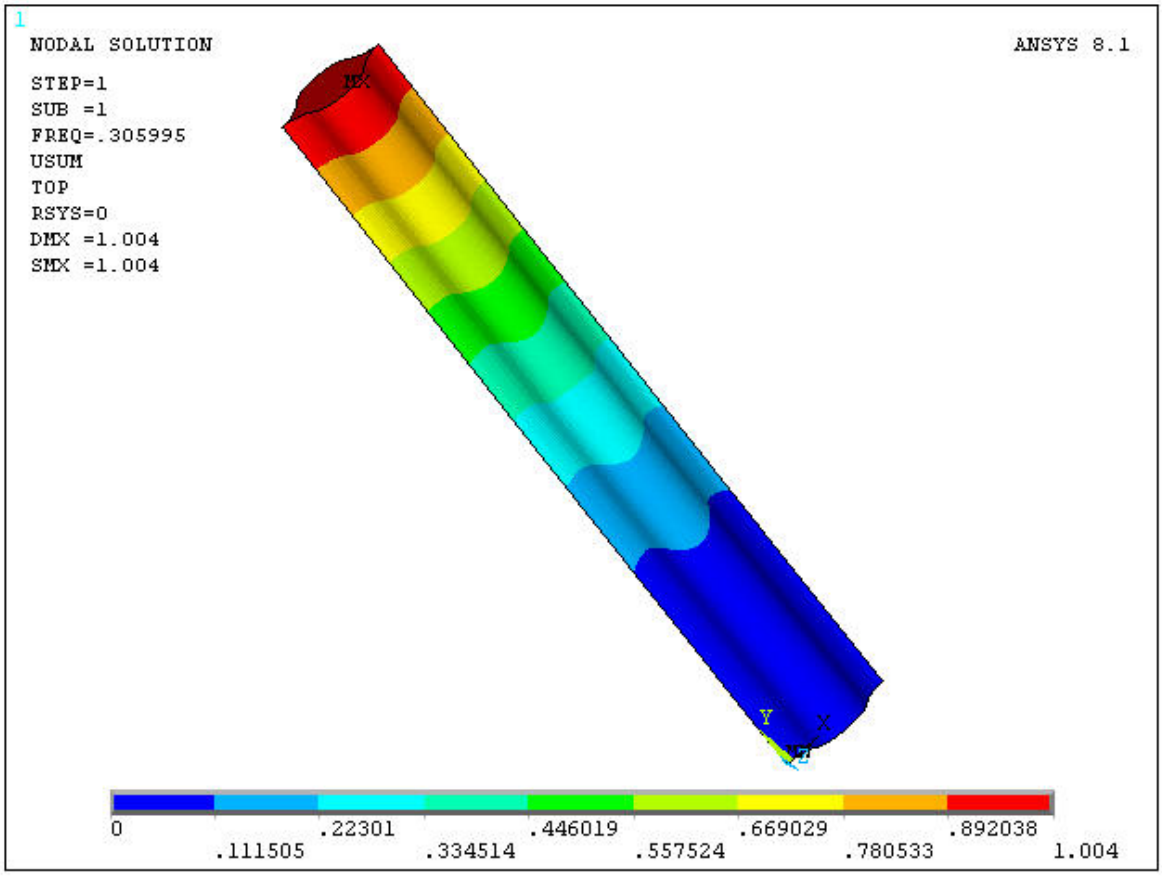

FIGURE 23

DISPLACEMENTS (MILLIMETRES) OF THERMOSETTING DEPLOYABLE BOOM (CLOSED SECTION)

PREPARED FOR

ESA, ESTEC
Noordwijk, The Netherlands

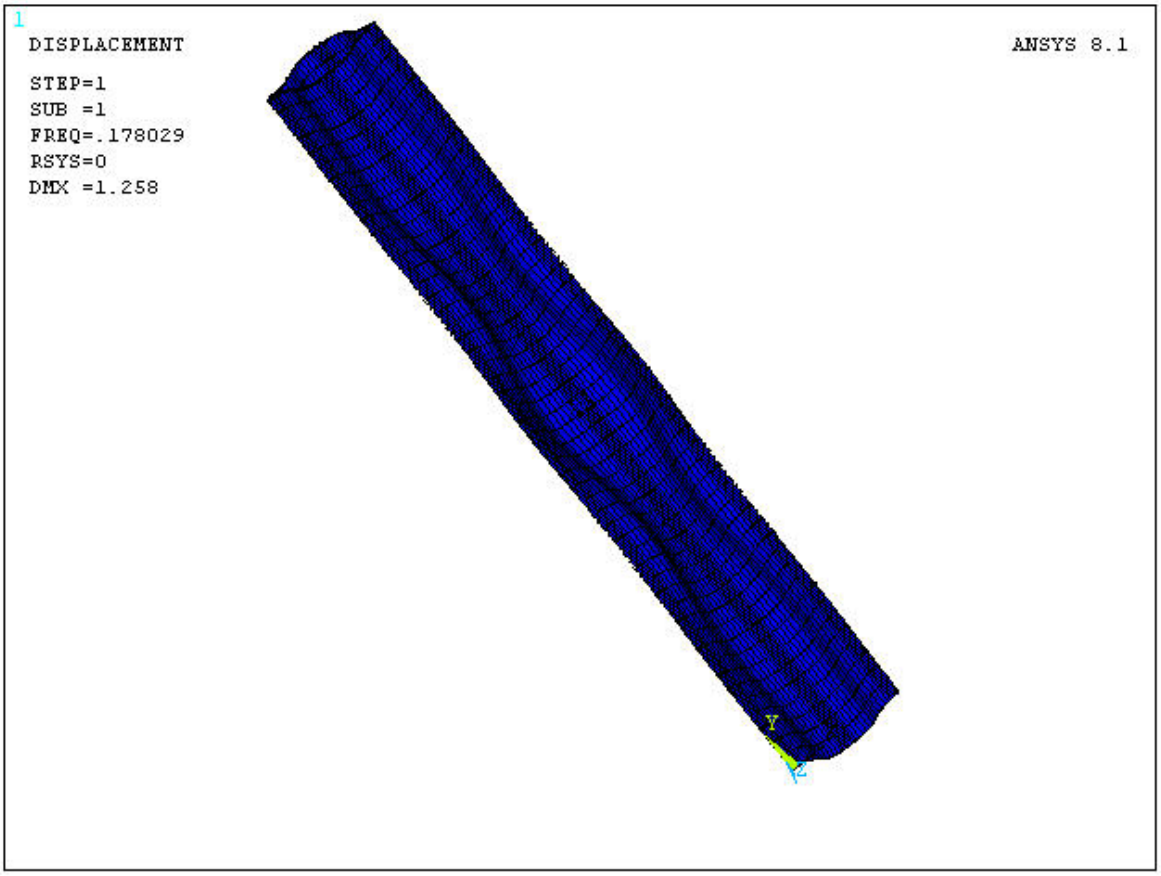

FIGURE 24

DEFORMED STRUCTURE OF
THERMOPLASTIC COMPOSITE BOOM
(CLOSED SECTION)

PREPARED FOR

ESA, ESTEC
Noordwijk, The Netherlands

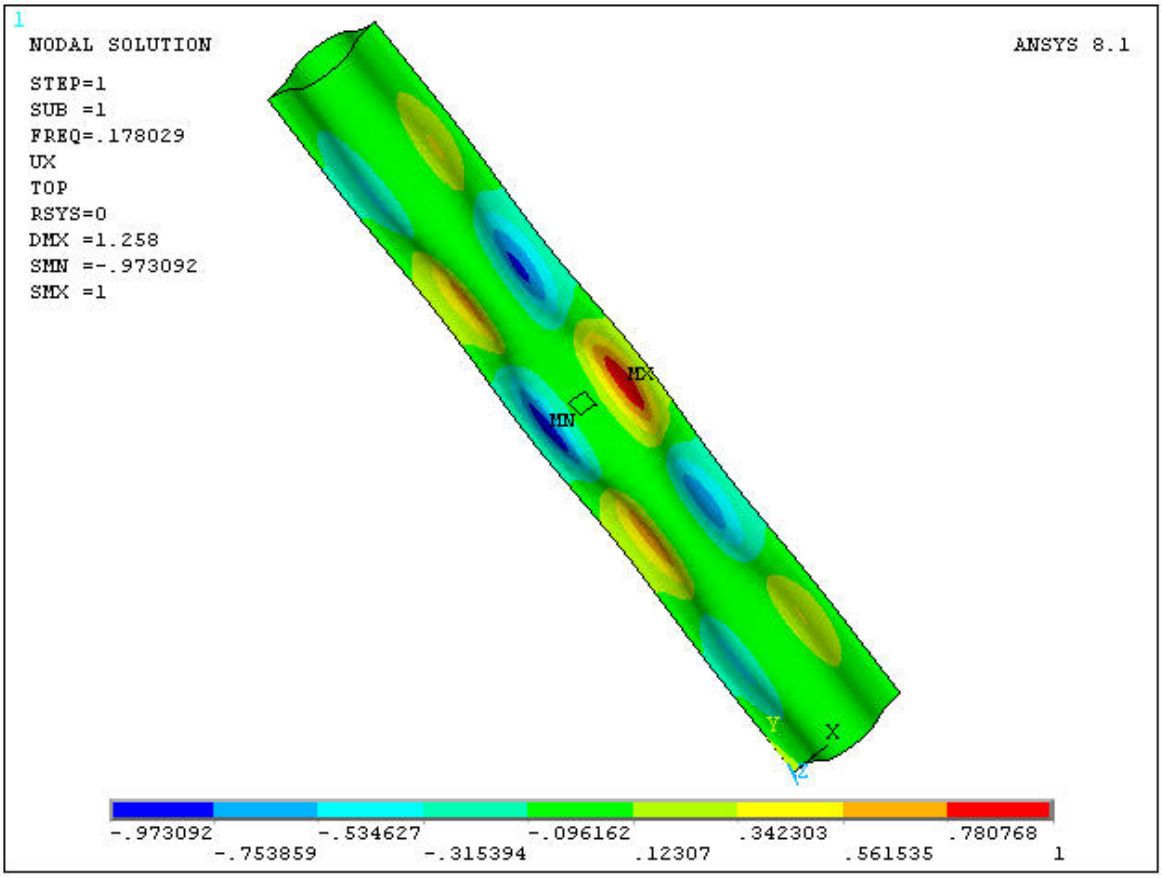

FIGURE 25

DISPLACEMENTS (MILLIMETRES) ALONG DIRECTION X OF THERMOPLASTIC DEPLOYABLE BOOM (CLOSED SECTION).

PREPARED FOR

ESA, ESTEC
Noordwijk, The Netherlands

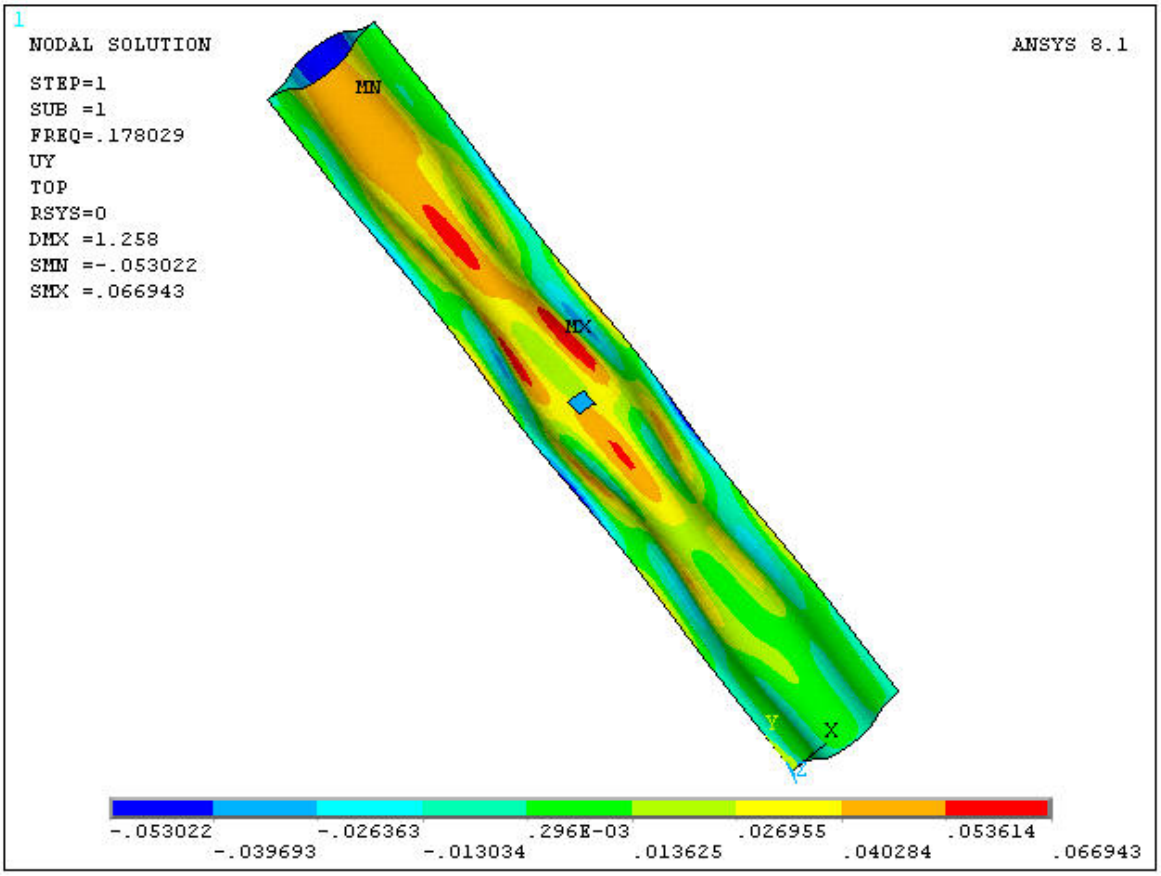

FIGURE 26

DISPLACEMENTS ALONG Y (MILLIMETRES)
OF THERMOPLASTIC DEPLOYABLE BOOM
(CLOSED SECTION)

PREPARED FOR

ESA, ESTEC
Noordwijk, The Netherlands

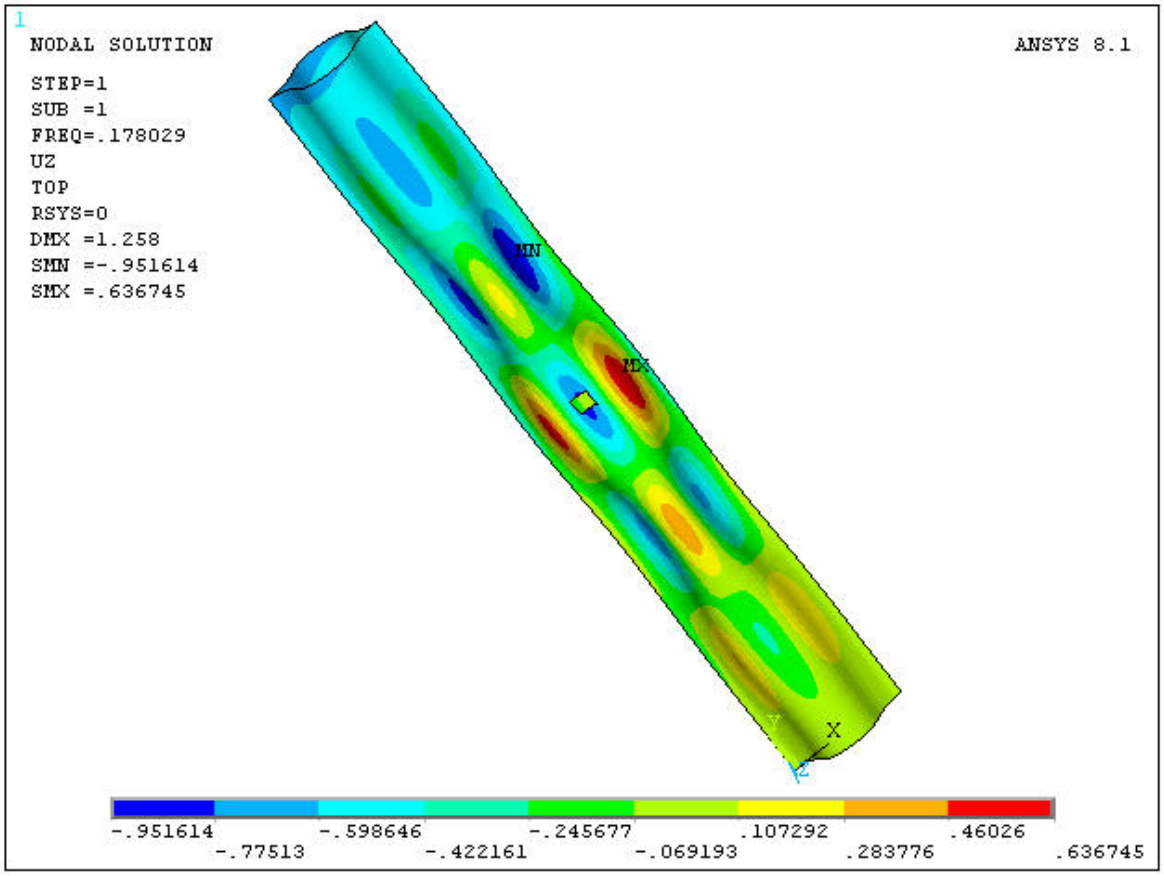

FIGURE 27

DISPLACEMENTS ALONG Z (MILLIMETRES)
OF THERMOPLASTIC DEPLOYABLE BOOM
(CLOSED SECTION)

PREPARED FOR

ESA, ESTEC
Noordwijk, The Netherlands

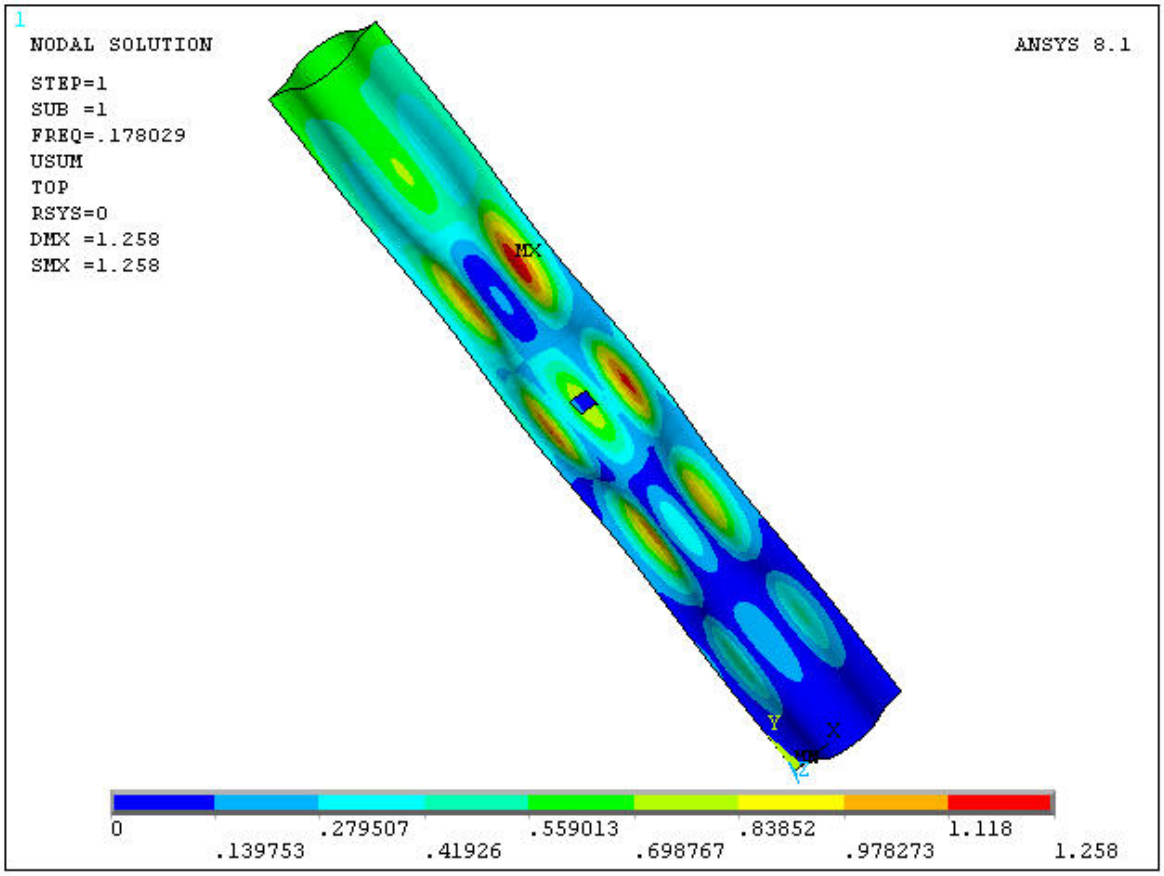

FIGURE 28

DISPLACEMENTS (MILLIMETRES) OF THERMOPLASTIC DEPLOYABLE BOOM (CLOSED SECTION)

PREPARED FOR

ESA, ESTEC
Noordwijk, The Netherlands

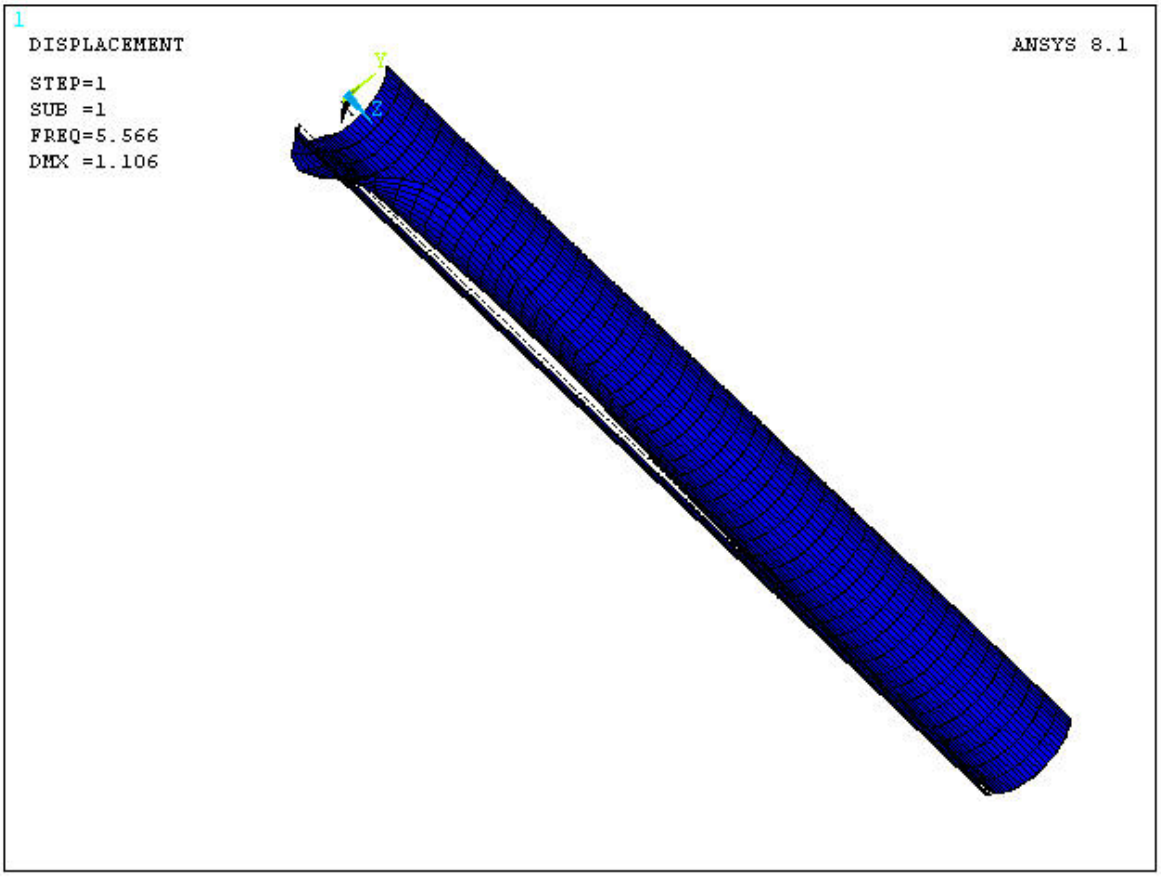

FIGURE 29

DEFORMED STRUCTURE OF
THERMOSETTING COMPOSITE BOOM
(OPEN SECTION)

PREPARED FOR

ESA, ESTEC
Noordwijk, The Netherlands

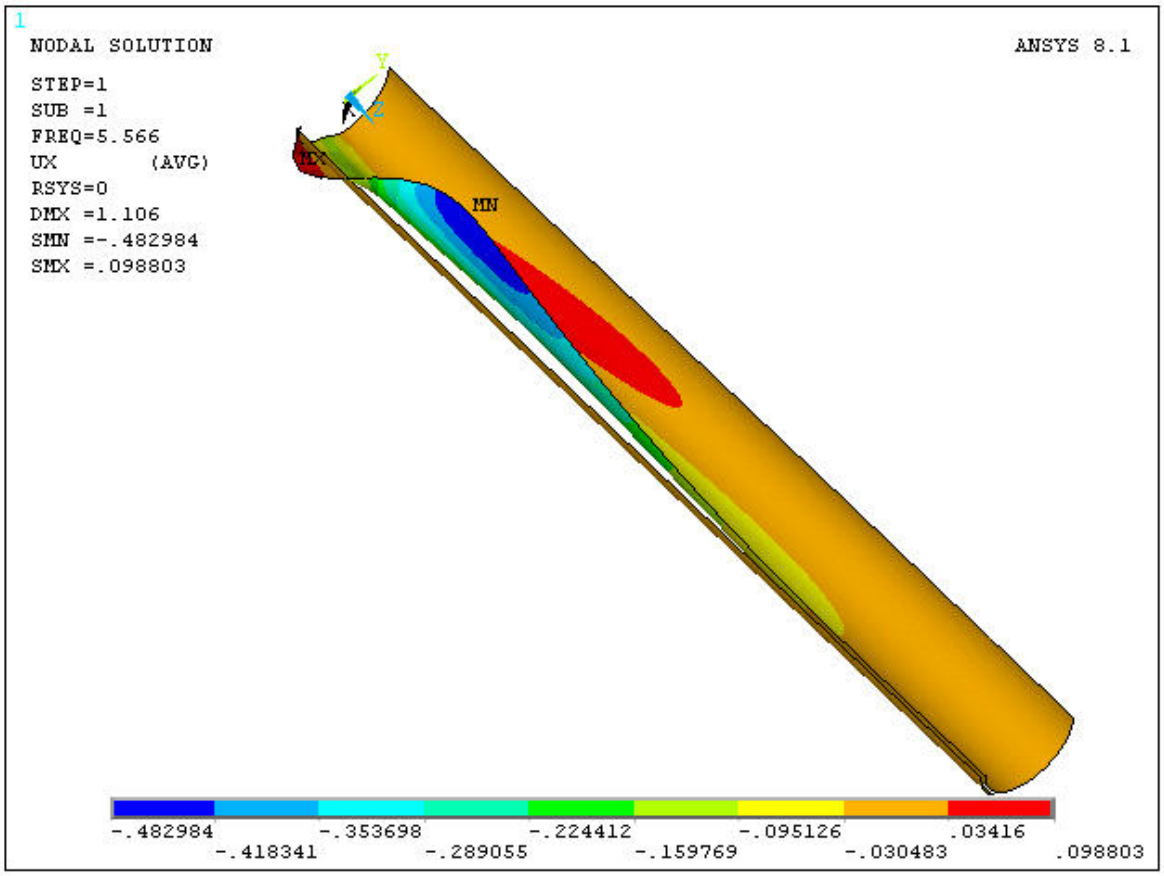

FIGURE 30

DISPLACEMENTS (MILLIMETRES) ALONG DIRECTION X OF THERMOSETTING DEPLOYABLE BOOM (OPEN SECTION)

PREPARED FOR

ESA, ESTEC
Noordwijk, The Netherlands

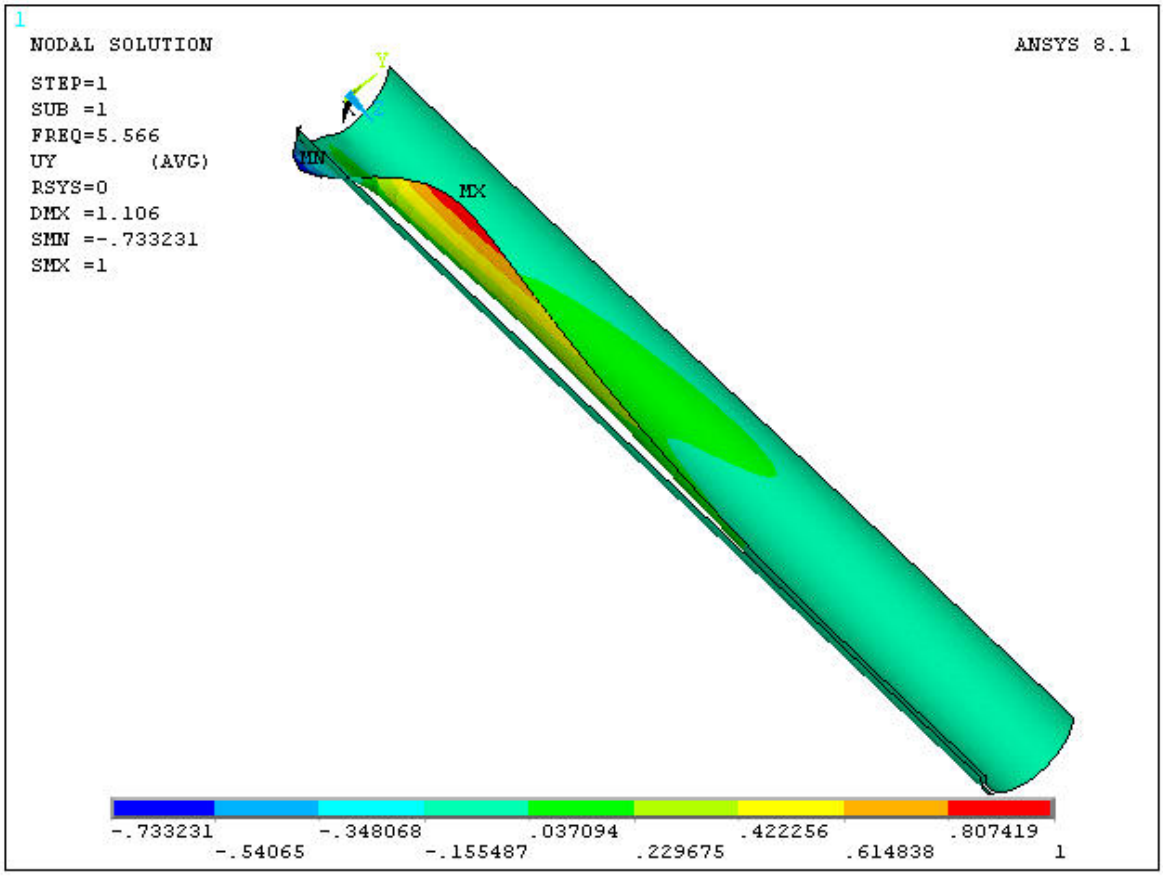

FIGURE 31

DISPLACEMENTS ALONG Y (MILLIMETRES)
OF THERMOSETTING DEPLOYABLE BOOM
(OPEN SECTION)

PREPARED FOR

ESA, ESTEC
Noordwijk, The Netherlands

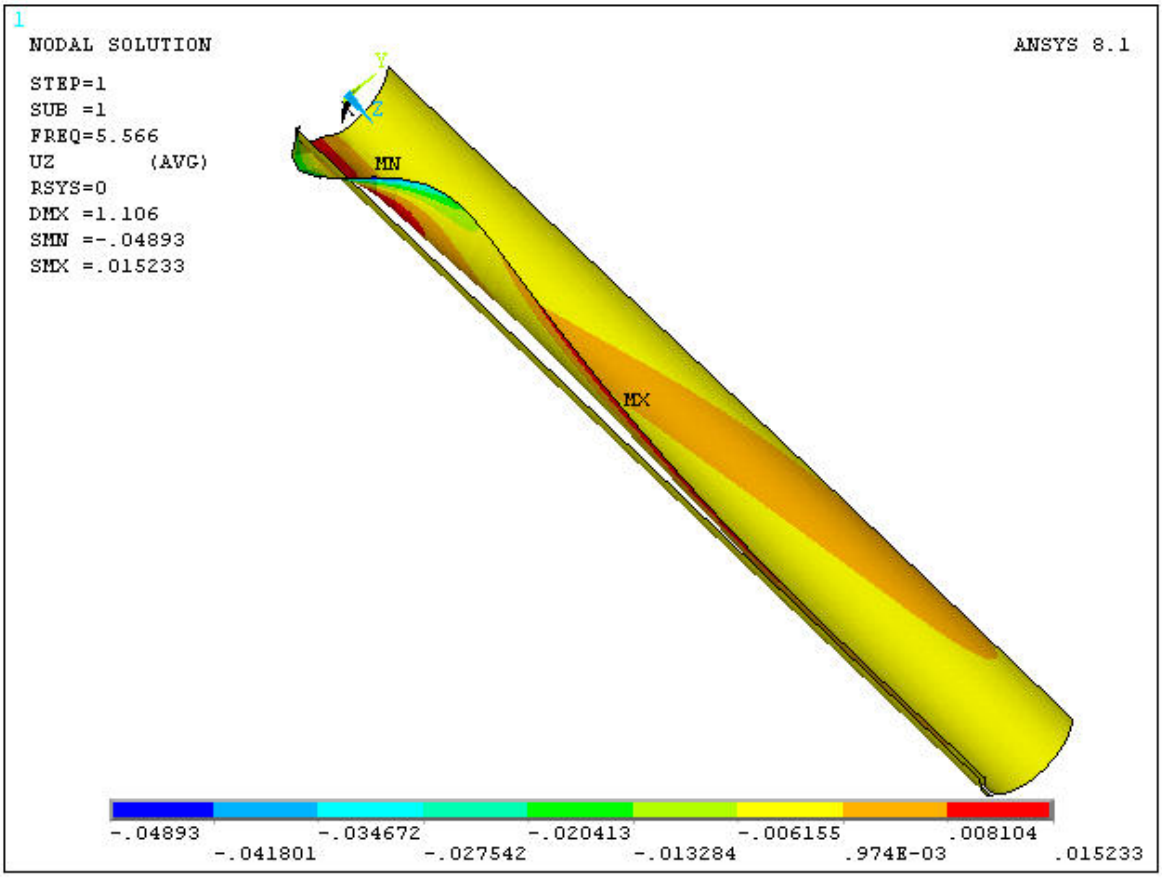

FIGURE 32

DISPLACEMENTS ALONG Z (MILLIMETRES)
OF THERMOSETTING DEPLOYABLE BOOM
(OPEN SECTION)

PREPARED FOR

ESA, ESTEC
Noordwijk, The Netherlands

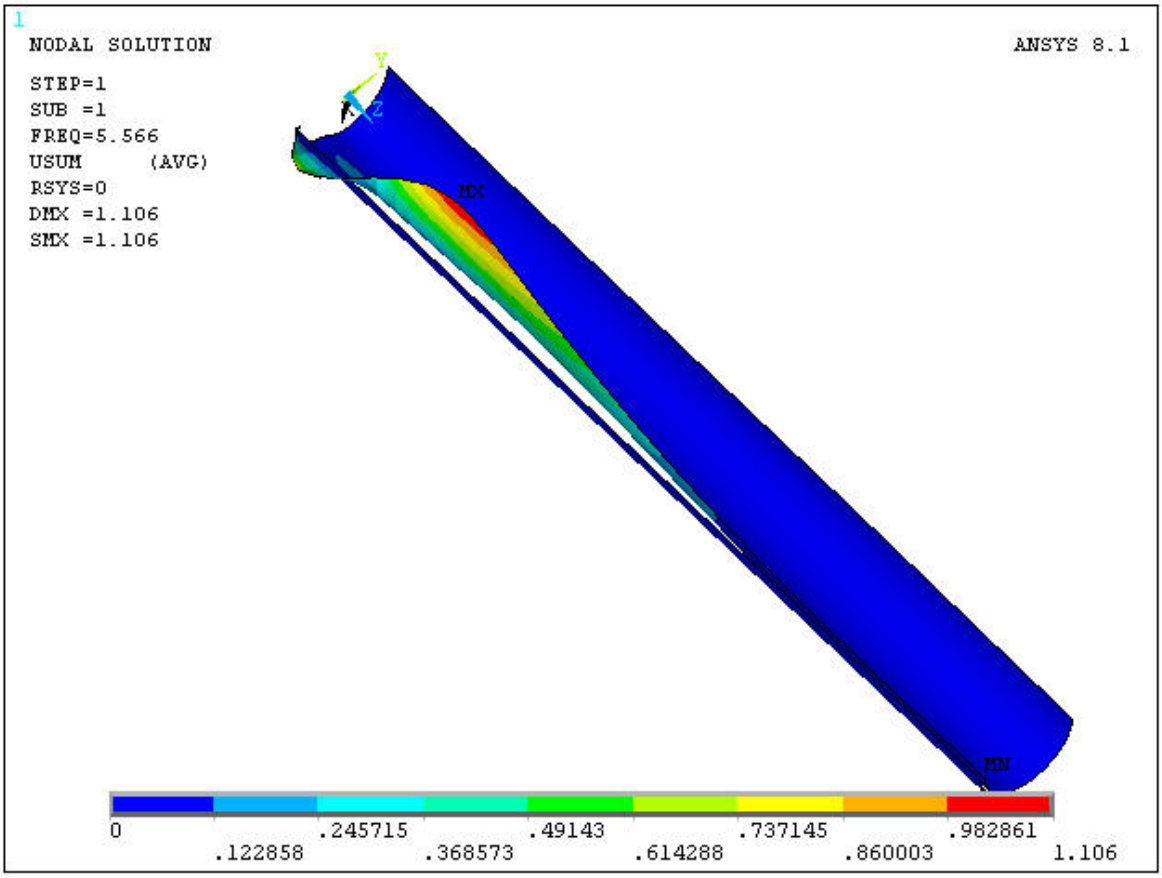

FIGURE 33

DISPLACEMENTS (MILLIMETRES) OF THERMOSETTING DEPLOYABLE BOOM (OPEN SECTION)

PREPARED FOR

ESA, ESTEC
Noordwijk, The Netherlands

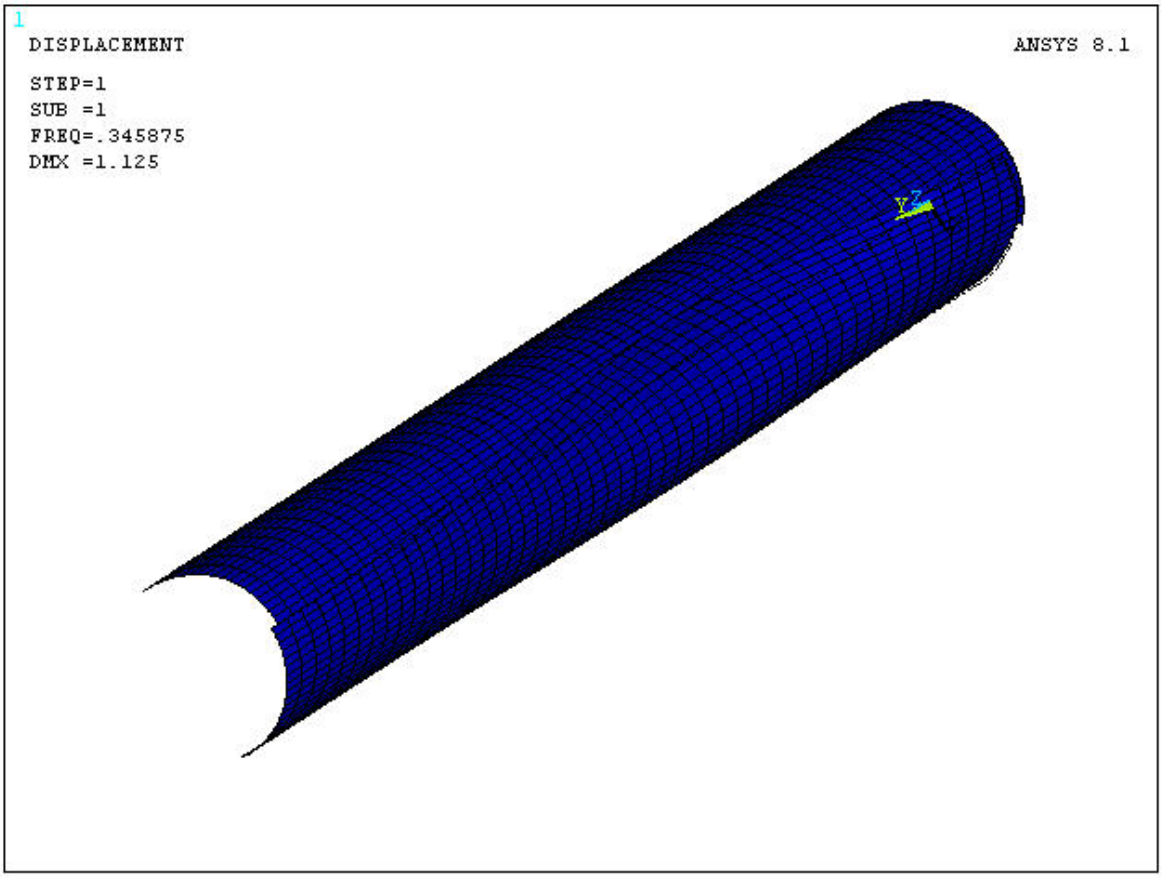

FIGURE 34

DEFORMED STRUCTURE OF
THERMOPLASTIC COMPOSITE BOOM
(OPEN SECTION)

PREPARED FOR

ESA, ESTEC
Noordwijk, The Netherlands

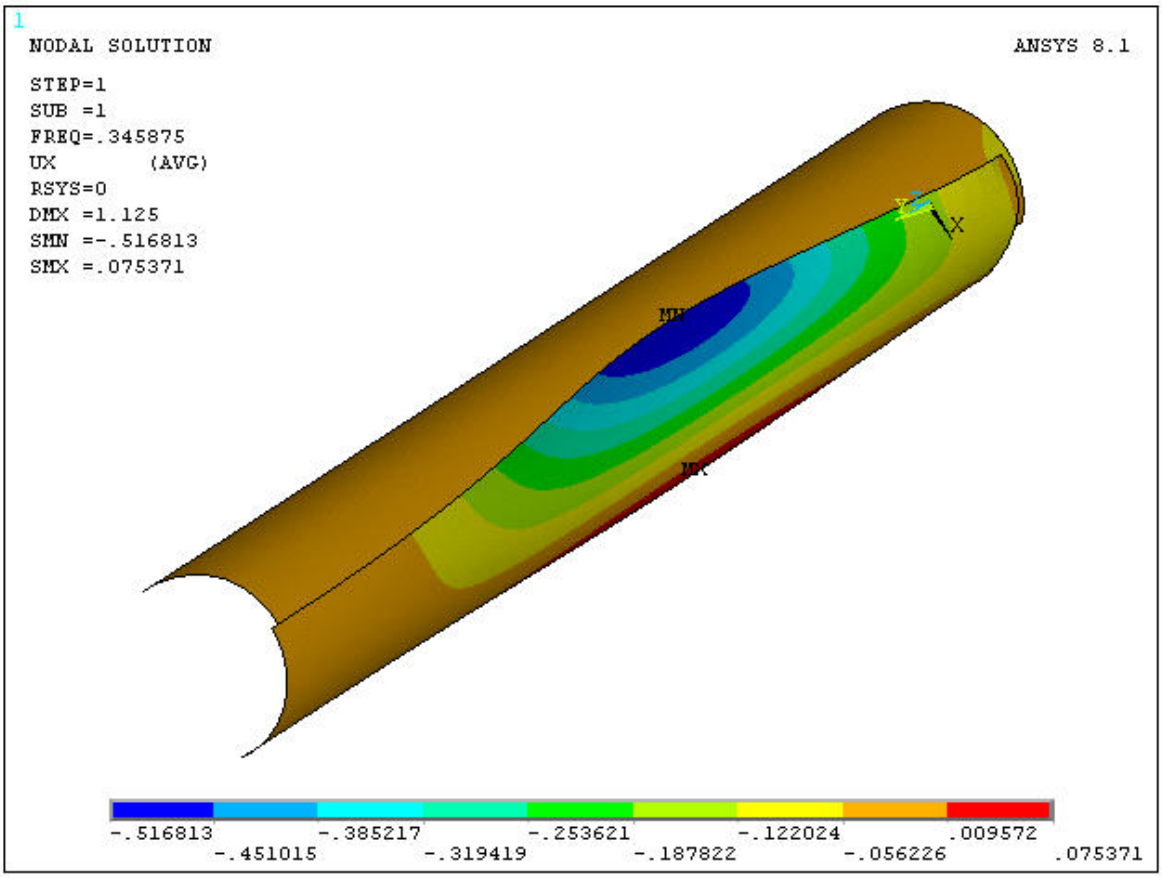

FIGURE 35

DISPLACEMENTS (MILLIMETRES) ALONG DIRECTION X OF THERMOPLASTIC DEPLOYABLE BOOM (COPEN SECTION)

PREPARED FOR

ESA, ESTEC
Noordwijk, The Netherlands

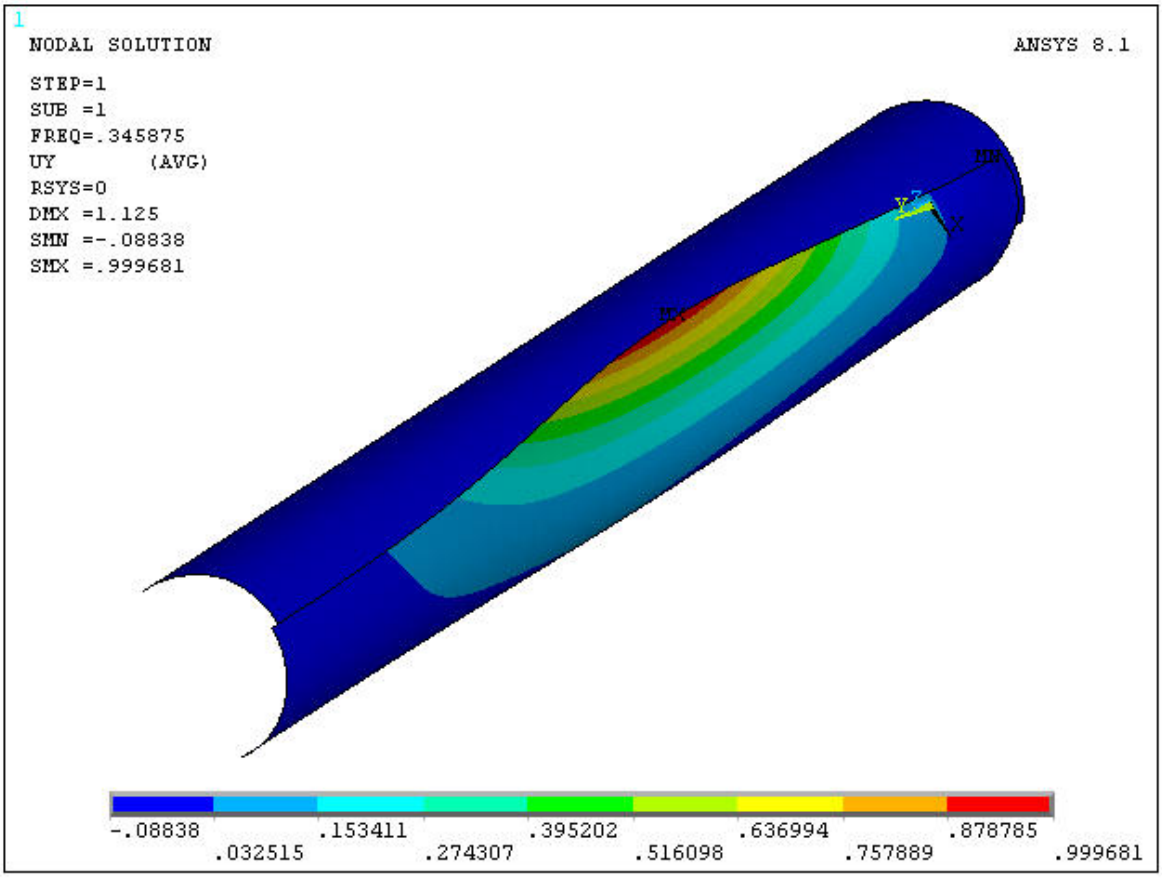

FIGURE 36

DISPLACEMENTS ALONG Y (MILLIMETRES)
OF THERMOSETTING DEPLOYABLE BOOM
(CLOSED SECTION)

PREPARED FOR

ESA, ESTEC
Noordwijk, The Netherlands

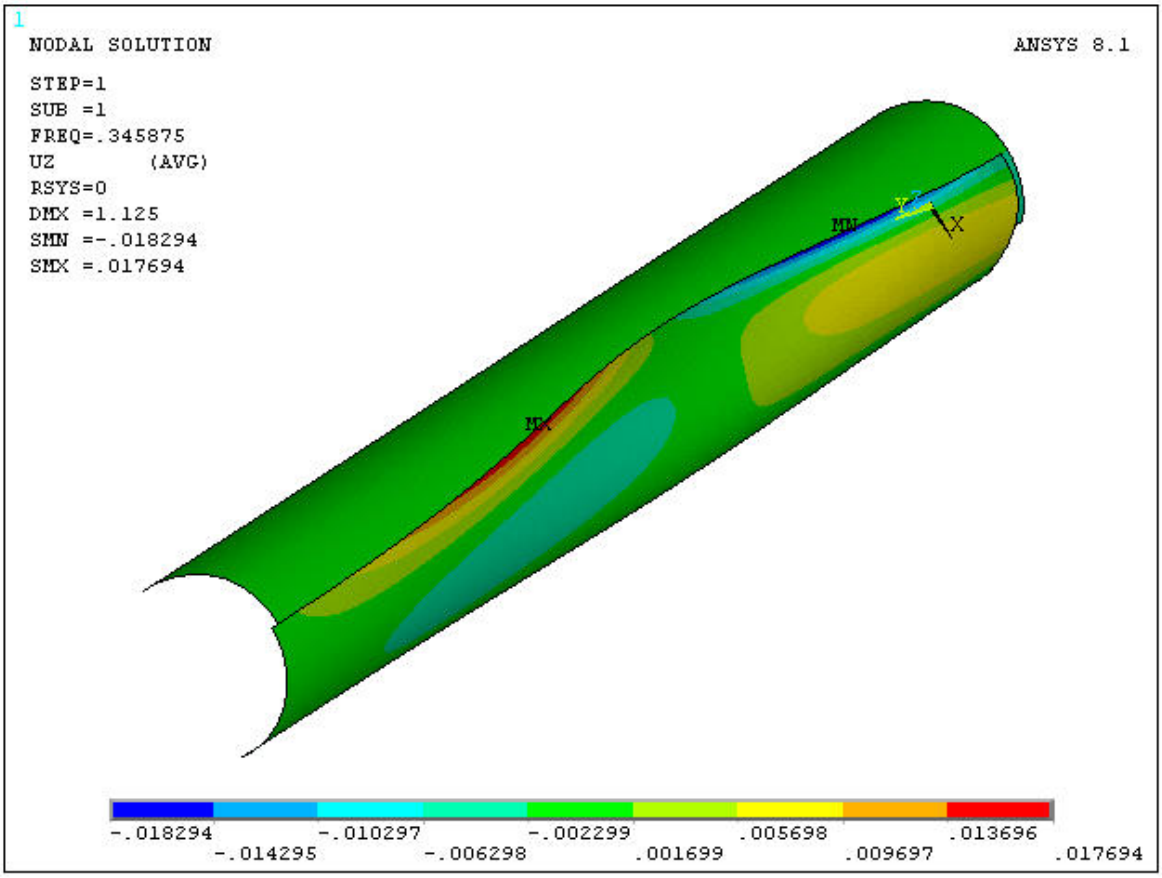

FIGURE 37

DISPLACEMENTS ALONG Z (MILLIMETRES)
OF THERMOSETTING DEPLOYABLE BOOM
(CLOSED SECTION)

PREPARED FOR

ESA, ESTEC
Noordwijk, The Netherlands

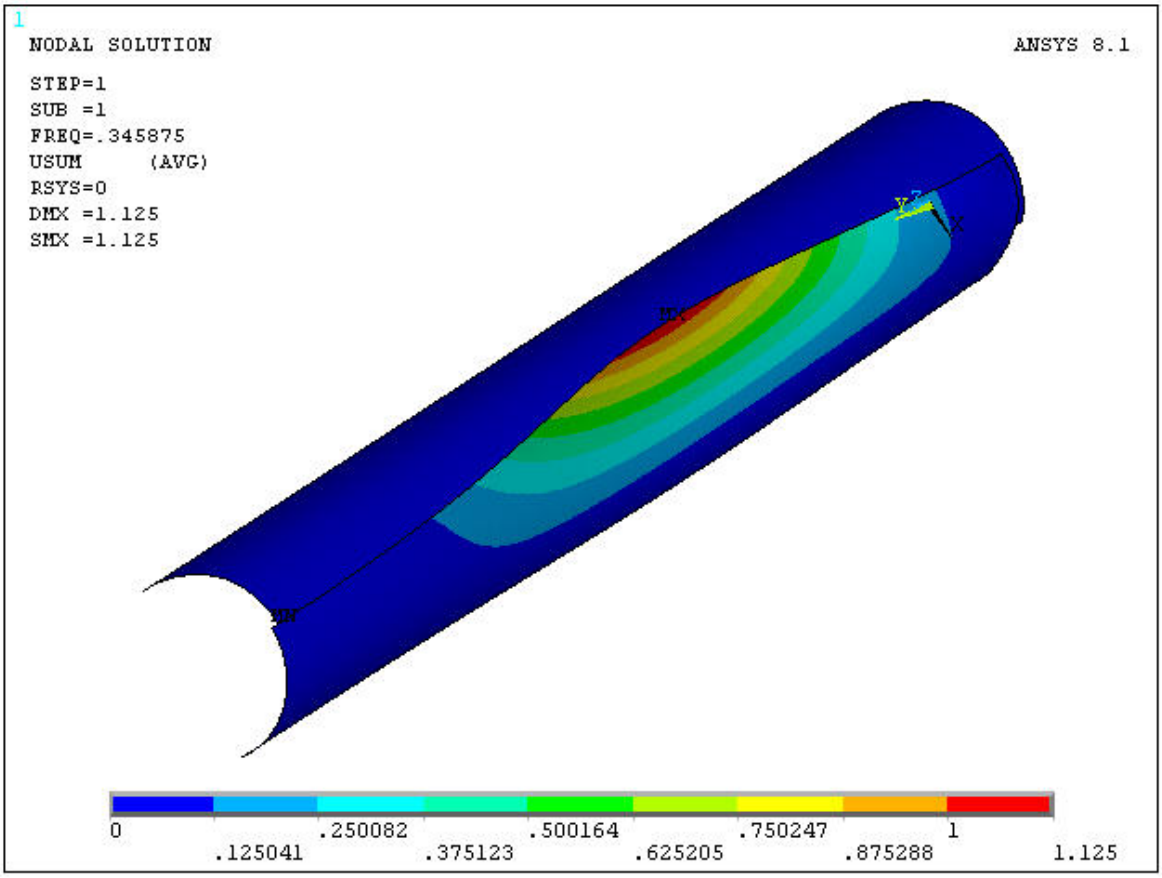

FIGURE 38

DISPLACEMENTS (MILLIMETRES) OF THERMOSETTING DEPLOYABLE BOOM (CLOSED SECTION)

PREPARED FOR

ESA, ESTEC
Noordwijk, The Netherlands